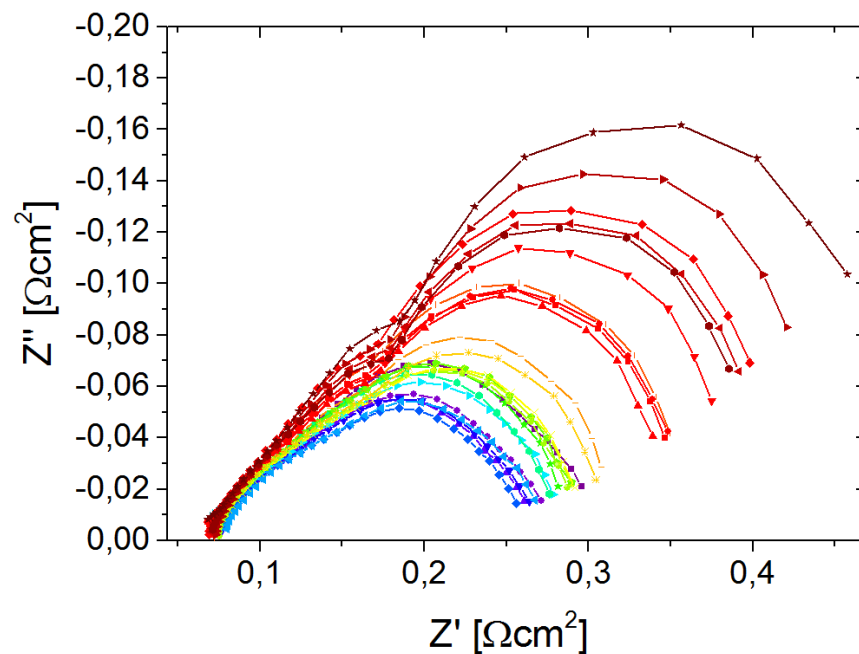


CHARACTERIZATION OF PEM FUEL CELLS BY ELECTROCHEMICAL IMPEDANCE SPECTROSCOPY



Dietmar Gerteisen, Anne-Christine Scherzer, Stefan Keller

Fraunhofer-Institut für Solare
Energie Systeme ISE

Heraeus-Seminar: Next generation
polymer membrane fuel cells

2.-5. July 2017

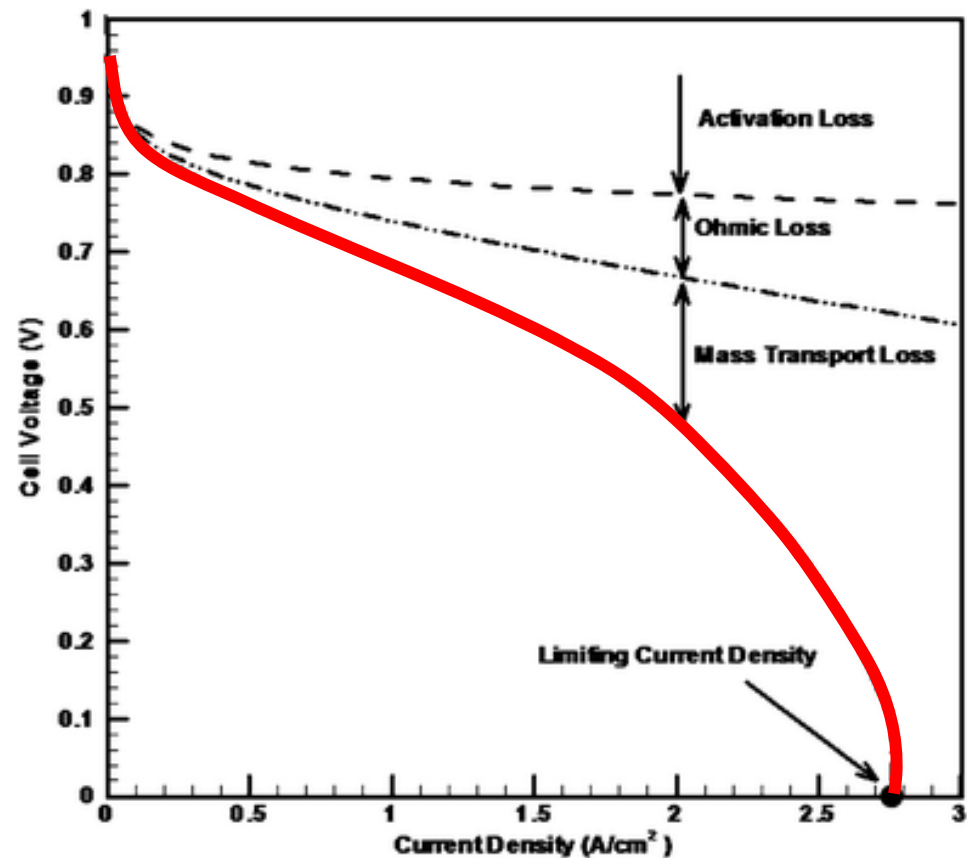
www.ise.fraunhofer.de

AGENDA

- Motivation: What can impedance spectra tell us?
- Characteristics of EIS and their interpretation
 - High frequency resistance (HFR)
 - 45°-branch at high frequencies
 - Charge transfer resistance
 - Mass transport resistance
- Differential cell measurements vs. „normal“ stoichiometric measurements
 - Channel impedance
- Conclusion

Interpretation of typical polarization curve

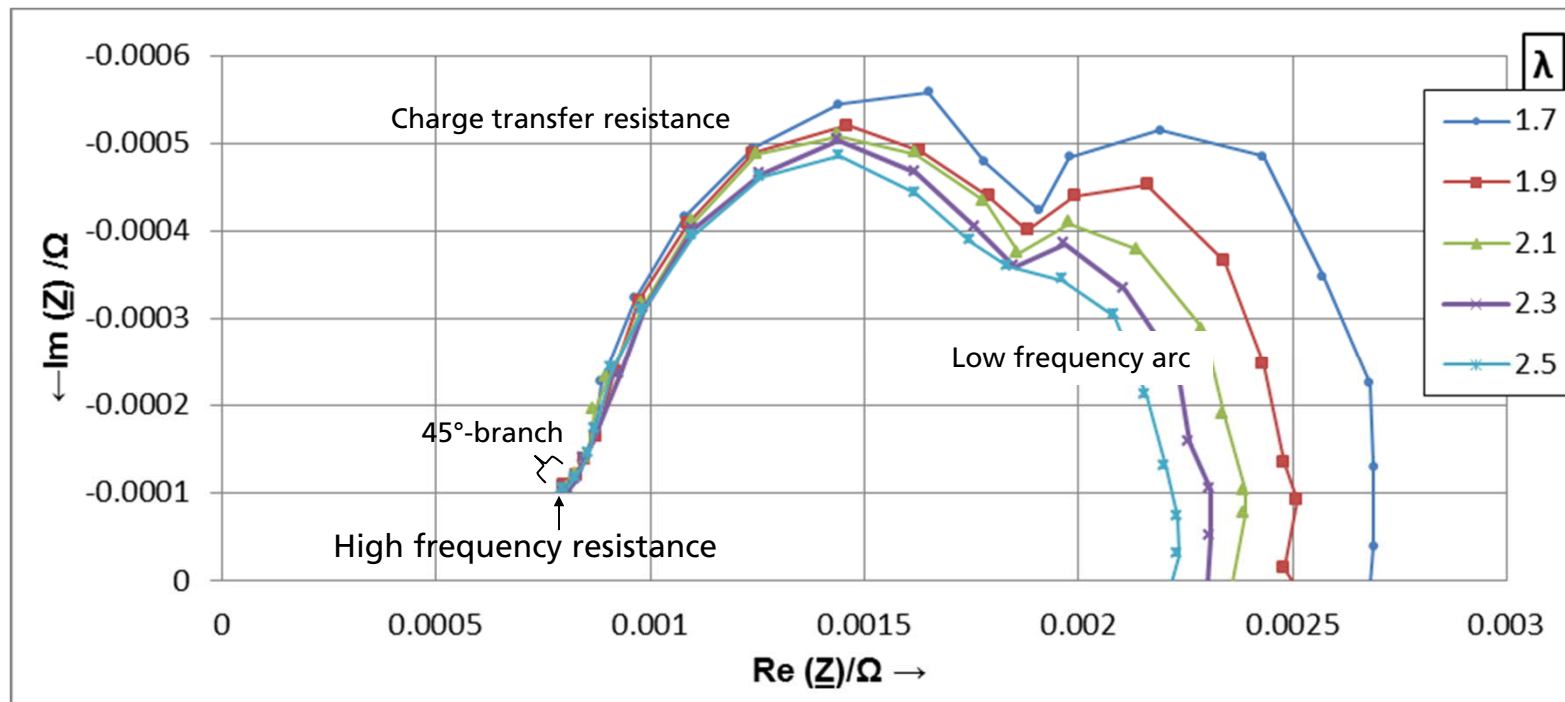
- PolCurve shows voltage at specific current
 - Voltage loss breakdown is of interest
- EIS can discriminate different loss mechanisms
 - if processes occur at different time constants



Mukerjee et al., Energy Environ. Sci., 2011, 4, 346-369

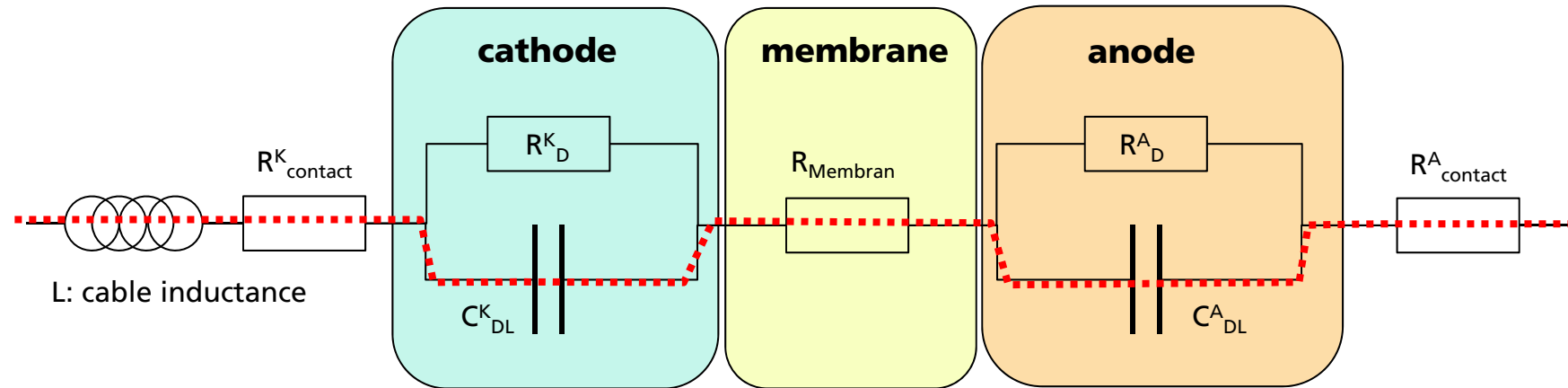
Typical impedance spectrum of a PEMFC stack

- Question: What can we learn from such spectra?



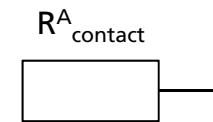
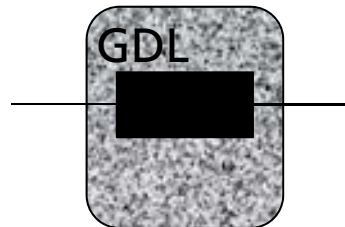
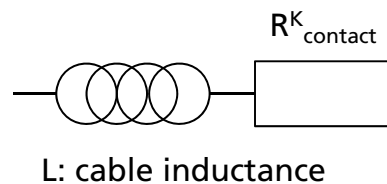
High frequency resistance

High frequency resistance (HFR)



$$Z_{FC}(\omega \rightarrow \infty) = i\omega L_{\text{cable}} + R^K_{\text{contact}} + R_{\text{membrane}} + R^A_{\text{contact}}$$

Der Hochfrequenzwiderstand (HFR)



$$Z_{\text{blank}}(\omega \rightarrow \infty) = i\omega L_{\text{cable}} + R^K_{\text{contact}} + R^A_{\text{contact}} + R_{\text{GDL}}$$

$$Z_{\text{FC}}(\omega \rightarrow \infty) - Z_{\text{blank}}(\omega \rightarrow \infty) = R_{\text{membrane}} - \cancel{R_{\text{GDL}}}$$

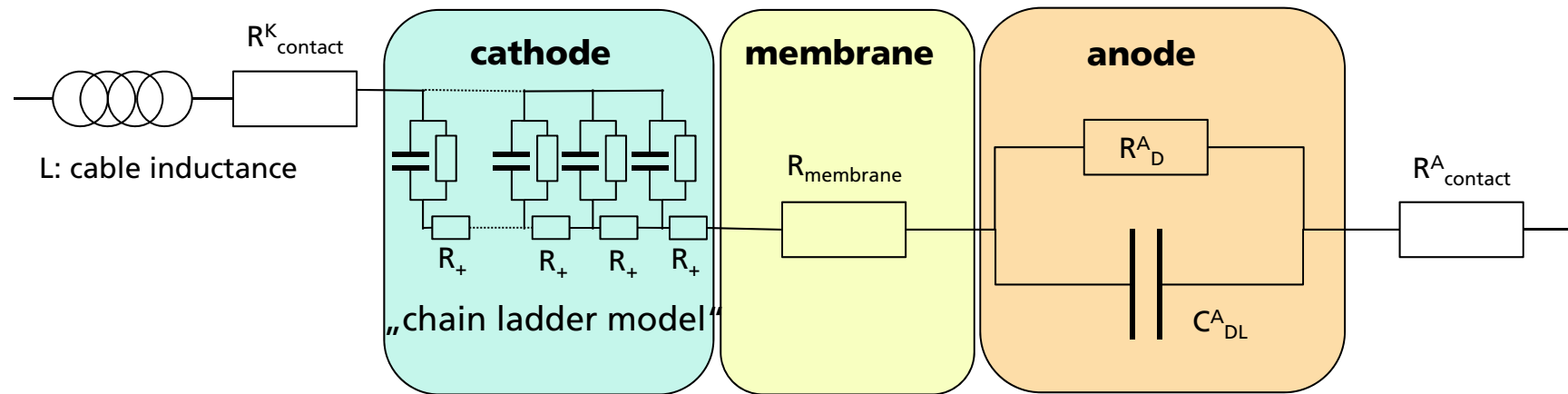
negligible or known

From HFR or conductivity, the membrane water content λ can be determined

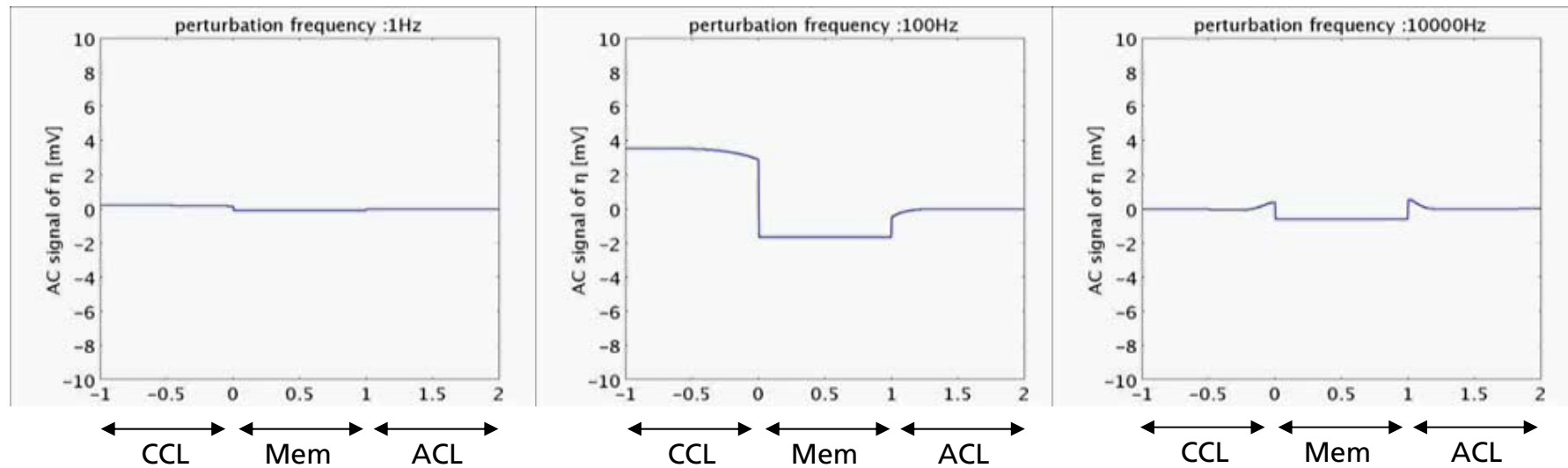
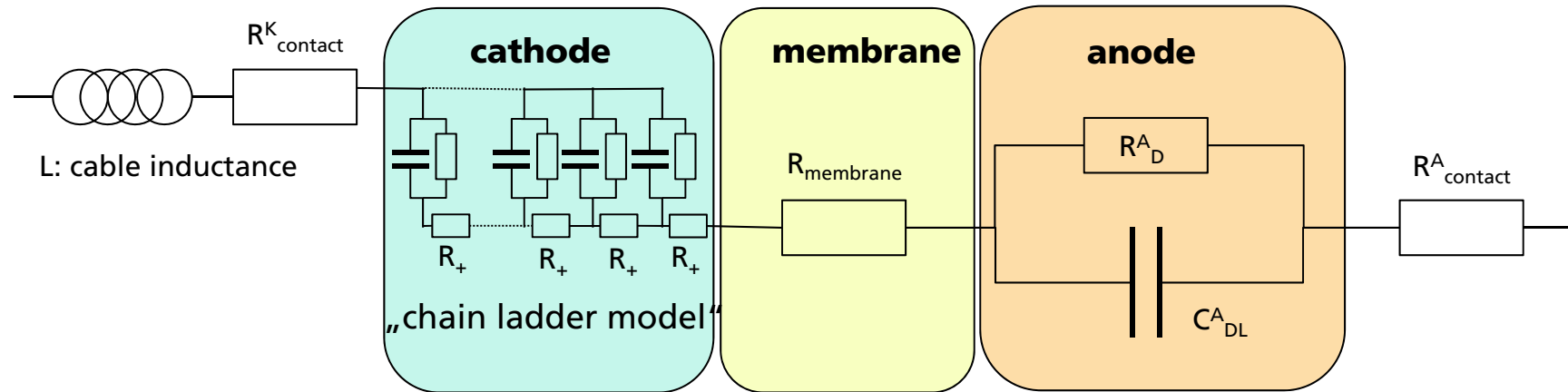
$$\sigma = (0.514 * \lambda - 0.326) e^{1268(\frac{1}{303} - \frac{1}{T})}$$

45°-branch and charge transfer resistance

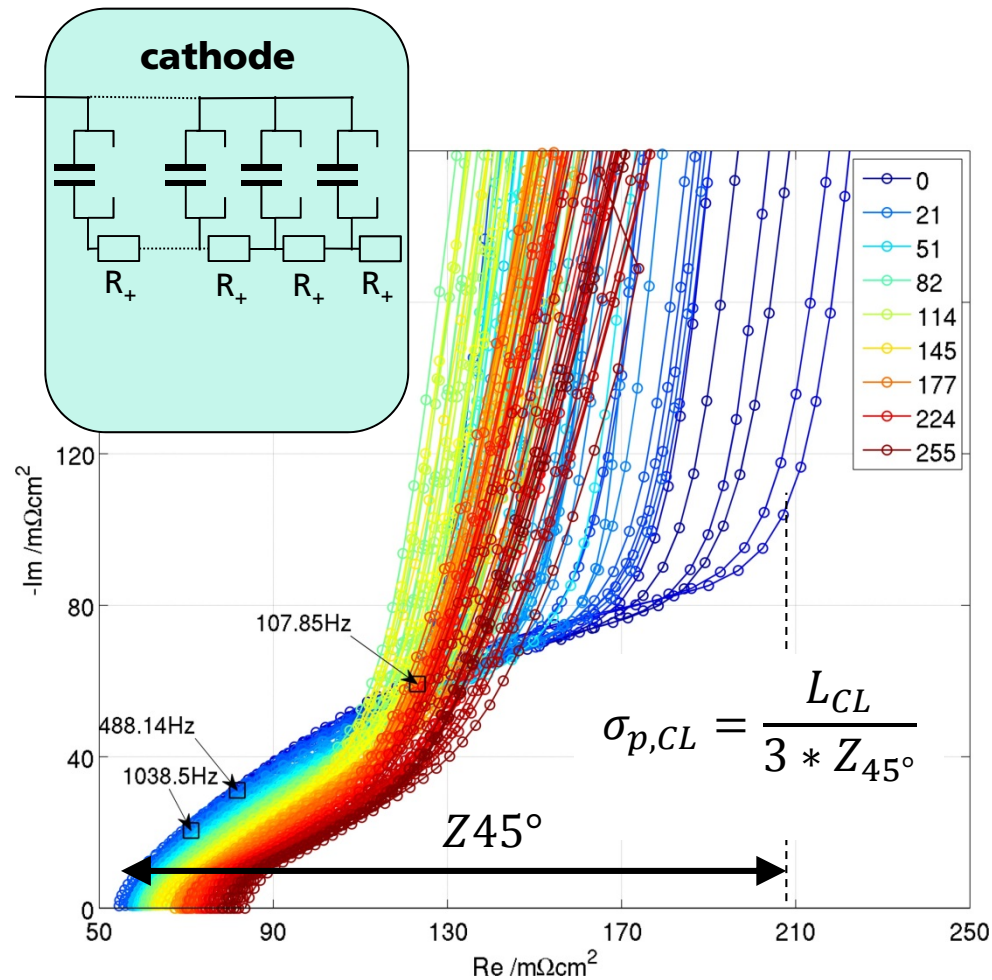
45°-branch @ high frequency



45°-branch @ high frequency

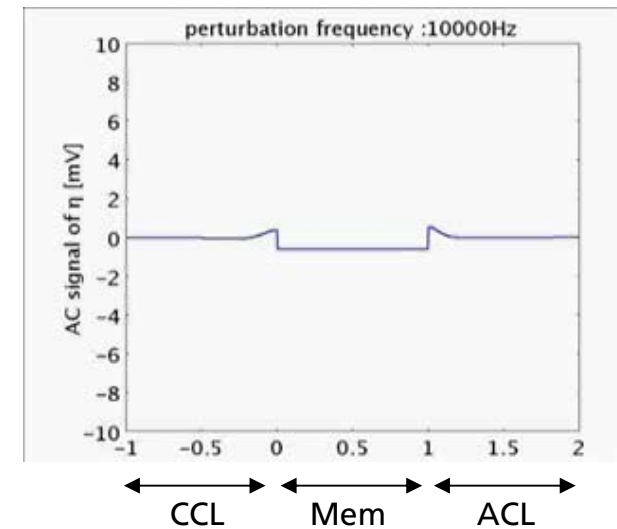


45°-branch @ high frequency



Example:

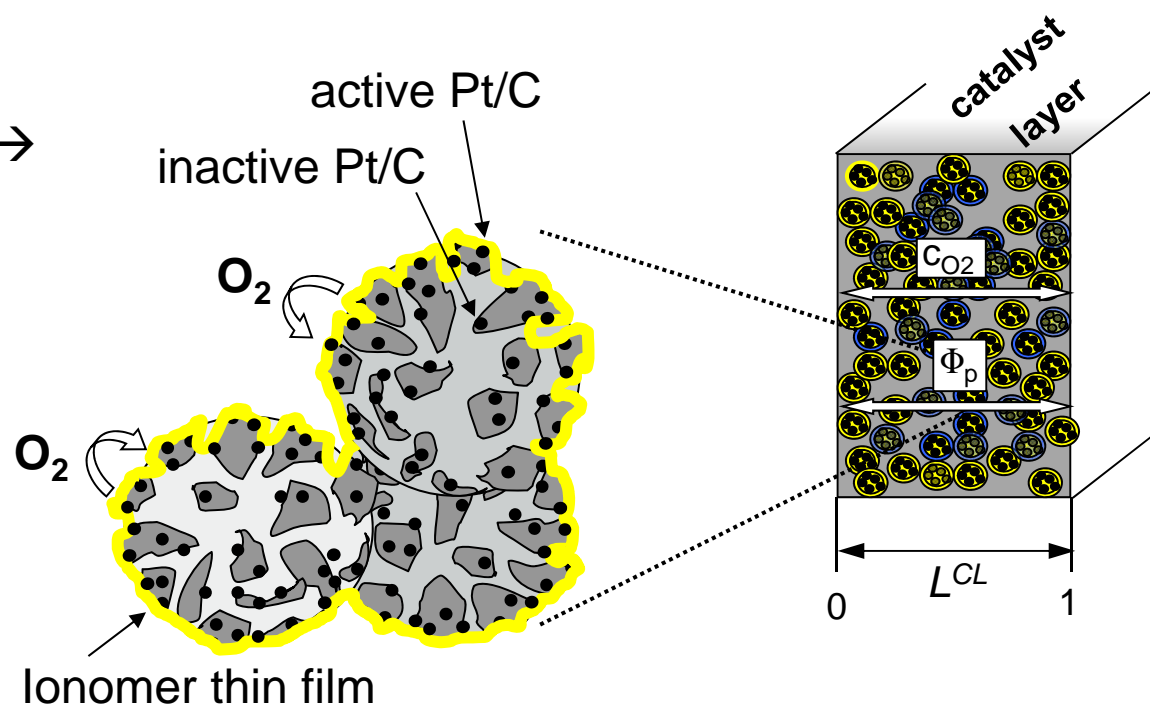
- EIS @ N_2/H_2
- Protonic resistance of CL



45°-branch @ high frequency

Inhomogeneous CL properties

- Agglomerate model
- Oxygen transport in CCL → concentration gradient dependent on D_{eff}
- Proton transport in CCL → overpotential gradient dependent on σ_{eff}



1D cathode model

- Charge balance equation & boundary conditions

$$l_{CL}^2 C_{DL} \frac{\partial(\Phi^p - \Phi^e)}{\partial t} - \frac{\partial}{\partial x} \left(\sigma \frac{\partial \Phi^p}{\partial x} \right) = -l_{CL}^2 \Lambda j_{gen}^a$$

$$\frac{\partial \Phi^p(0)}{\partial x} = 0 \qquad \Phi^p(1) = 0$$

- Mass balance equation & boundary conditions

$$l_{CL}^2 \varepsilon_{CL}^{eff} \frac{\partial c_{O_2}}{\partial t} - \frac{\partial}{\partial x} \left(D_{O_2}^{eff} \frac{\partial c_{O_2}}{\partial x} \right) = -l_{CL}^2 \frac{\Lambda}{4F} j_{gen}^a$$

$$c_{O_2}(0) = c_{O_2}^{GDL} \qquad \frac{\partial c_{O_2}(1)}{\partial x} = 0$$

1D cathode model

- Differential equation system after perturbation, linearization and Laplace transformation

$$l_{CL}^2 C_{DL} s (\overline{\Phi^p} - \overline{\Phi^e}) - \frac{\partial}{\partial x} \left(\sigma \frac{\partial \overline{\Phi^p}}{\partial x} \right) = -l_{CL}^2 \Lambda \overline{j_{gen}^a}$$

$$l_{CL}^2 \varepsilon_{CL}^{eff} s \overline{c_{O_2}} - \frac{\partial}{\partial x} \left(D_{O_2}^{eff} \frac{\partial \overline{c_{O_2}}}{\partial x} \right) = -l_{CL}^2 \frac{\Lambda}{4F} \overline{j_{gen}^a}$$

$$\overline{\Phi^p}(1) = \frac{\partial \overline{\Phi^p}(0)}{\partial x} = \frac{\partial \overline{c_{O_2}}(1)}{\partial x} = \overline{c_{O_2}}(0) = 0$$

$$Z = \frac{\overline{\Phi^e}}{\sigma \frac{\partial \overline{\Phi^p}(1)}{\partial x}}$$

What happens for inhomogeneous CL properties?

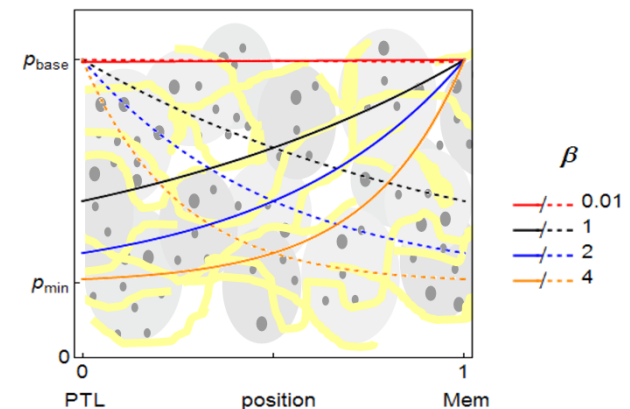
- Differential equation system after perturbation, linearization and Laplace transformation

$$l_{CL}^2 \underbrace{C_{DL}} (\overline{\Phi^p} - \overline{\Phi^e}) - \frac{\partial}{\partial x} \left(\underbrace{\sigma}_{\frac{\partial \overline{\Phi^p}}{\partial x}} \right) = -l_{CL}^2 \Lambda \overline{j_{gen}^a}$$

$$l_{CL}^2 \underbrace{\varepsilon_{CL}^{eff}} s \overline{c_{O2}} - \frac{\partial}{\partial x} \left(\underbrace{D_{O2}^{eff}} \frac{\partial \overline{c_{O2}}}{\partial x} \right) = -l_{CL}^2 \frac{\Lambda}{4F} \overline{j_{gen}^a}$$

$$\overline{\Phi^p}(1) = \frac{\partial \overline{\Phi^p}(0)}{\partial x} = \frac{\partial \overline{c_{O2}}(1)}{\partial x} = \overline{c_{O2}}(0) = 0$$

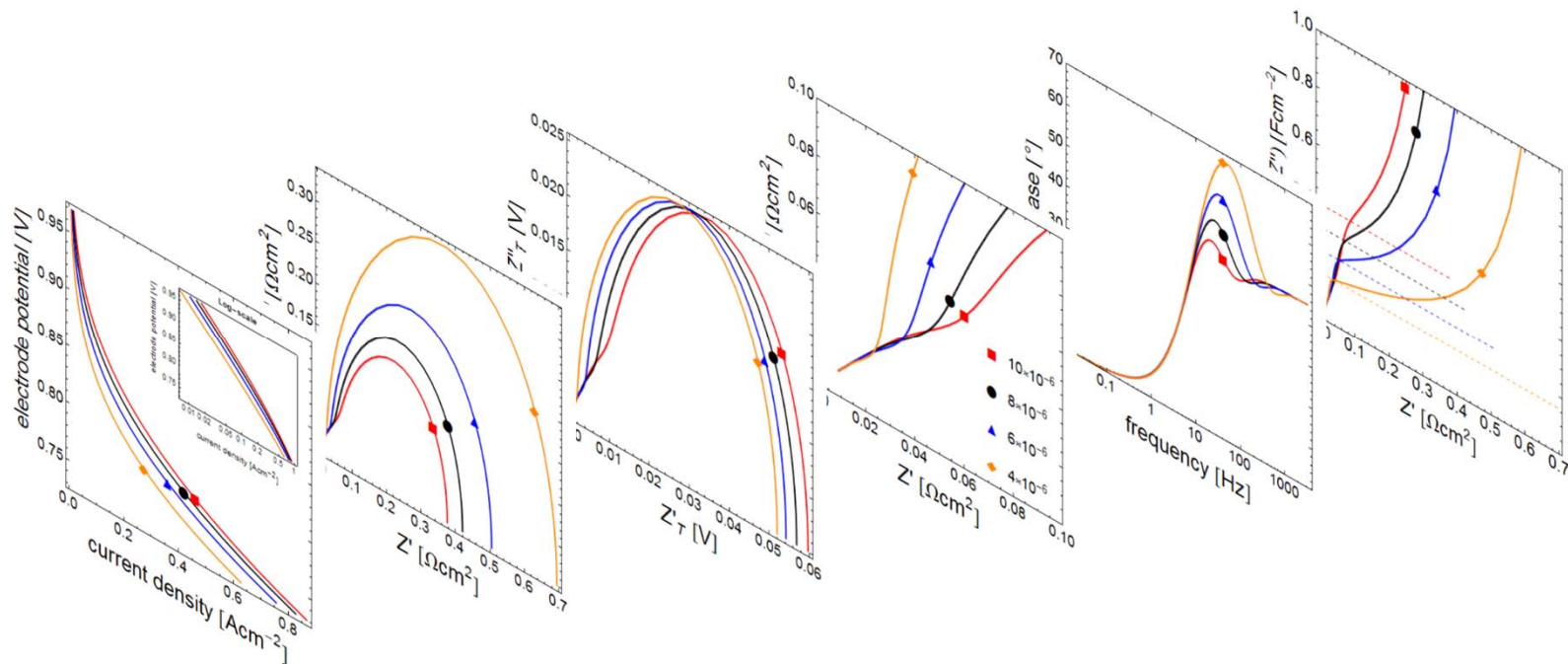
$$Z = \frac{\overline{\Phi^e}}{\sigma \frac{\partial \overline{\Phi^p}(1)}{\partial x}}$$



$$p(y) = p_{base}(\alpha + (1 - \alpha))e^{-\beta \cdot \tilde{y}}$$

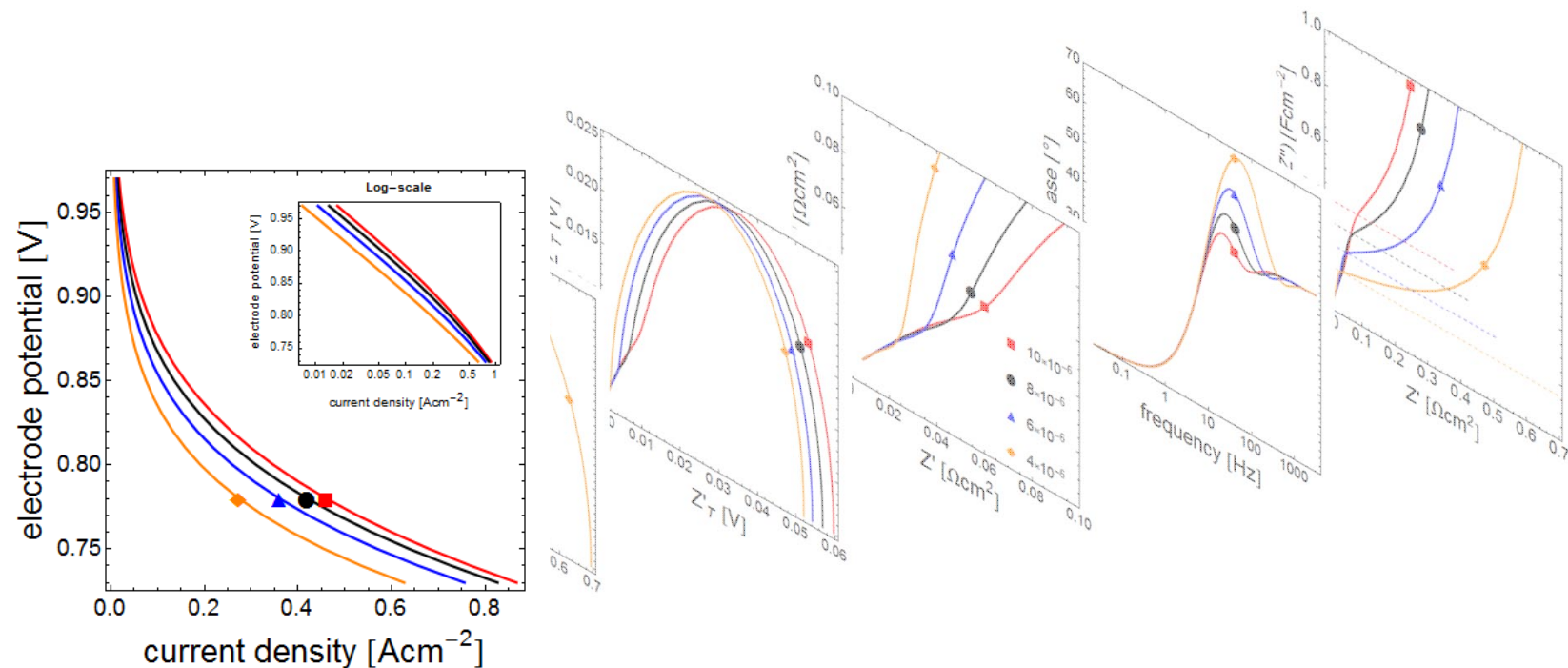
Variation of catalyst layer thickness

- Homogeneous CL properties !!



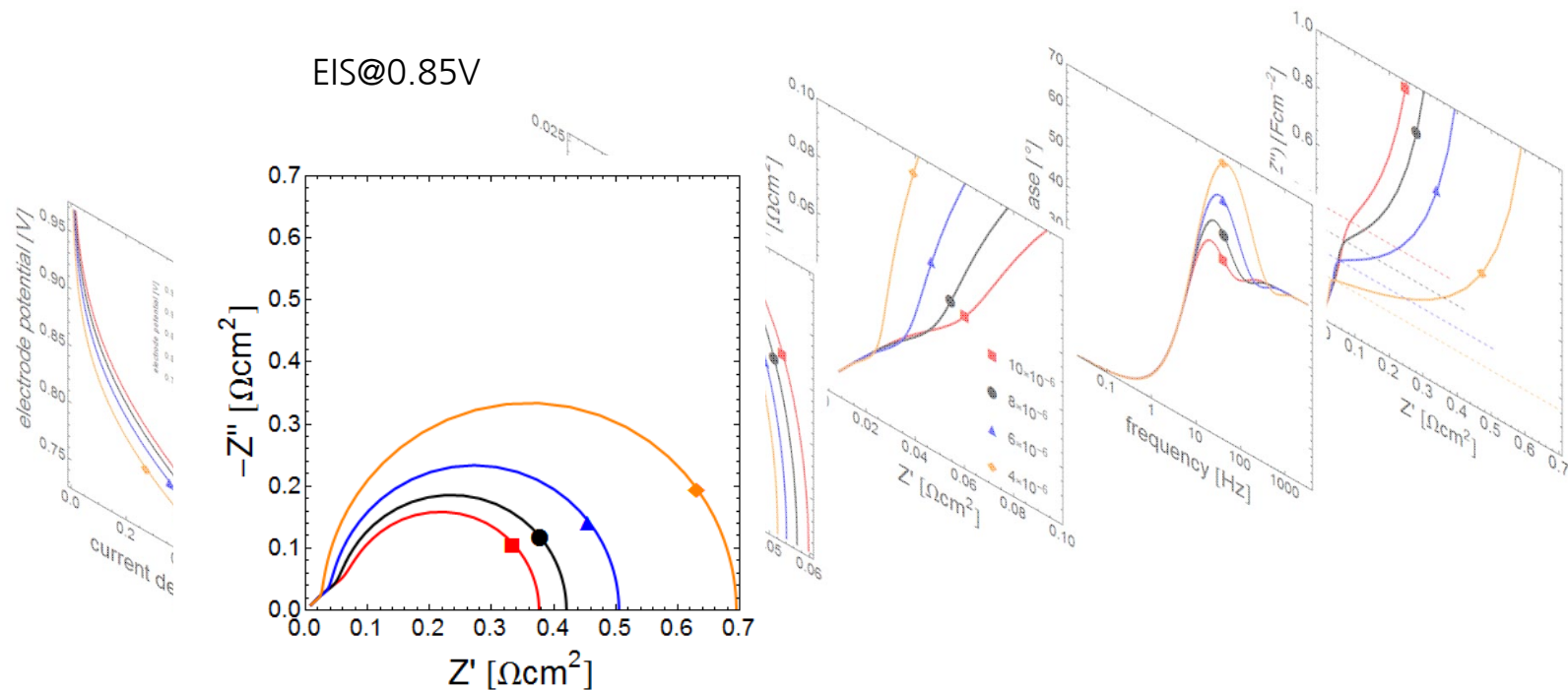
Variation of catalyst layer thickness

- Polarization curve
 - Doubling of Tafel slope for thicker CL at lower current density



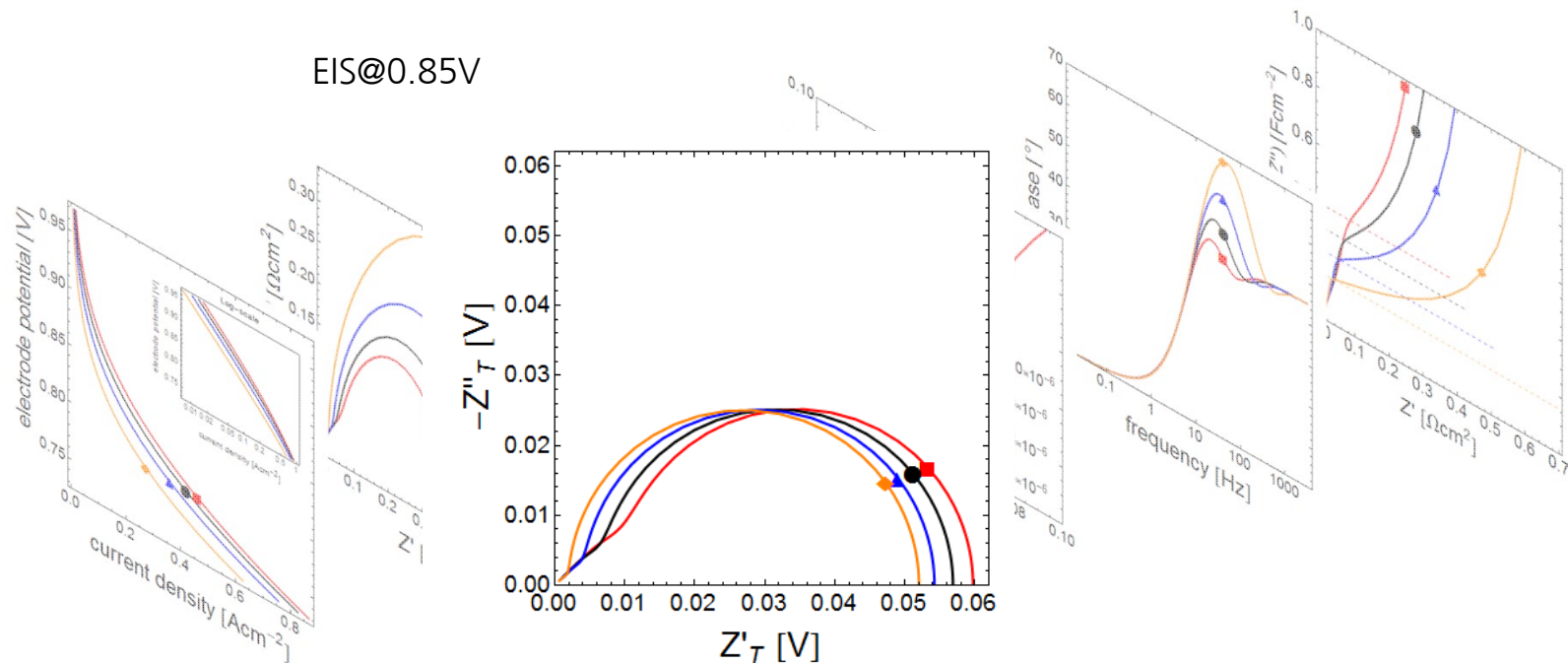
Variation of catalyst layer thickness

- Impedance spectra as Nyquist-Plot
 - R_{CT} increases with lowering the CL thickness



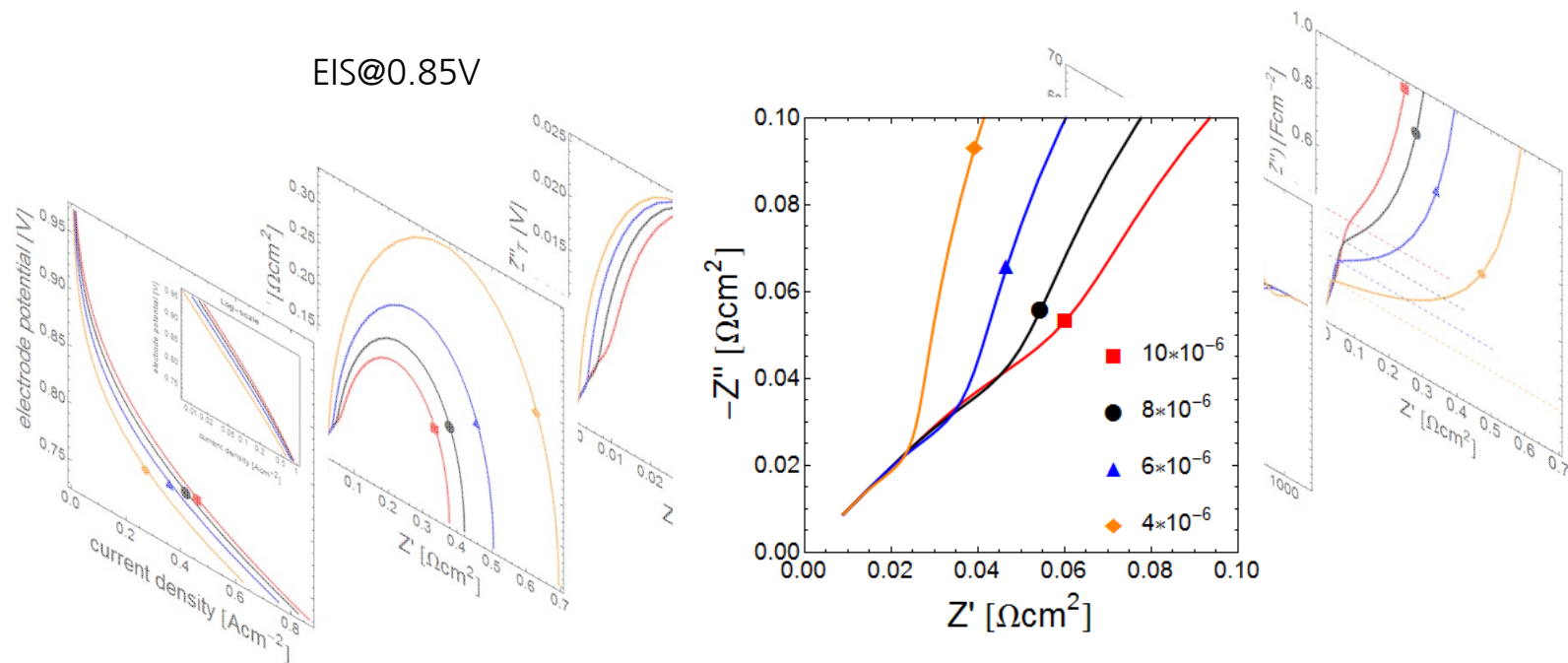
Variation of catalyst layer thickness

- Tafel-Impedance as Nyquist-Plot $\rightarrow Z_T = i_{\text{steady-state}} * Z$
 - Identical height \rightarrow Tafel slope identical
 - Shift to higher real part due to larger 45° branch (scales with thickness)



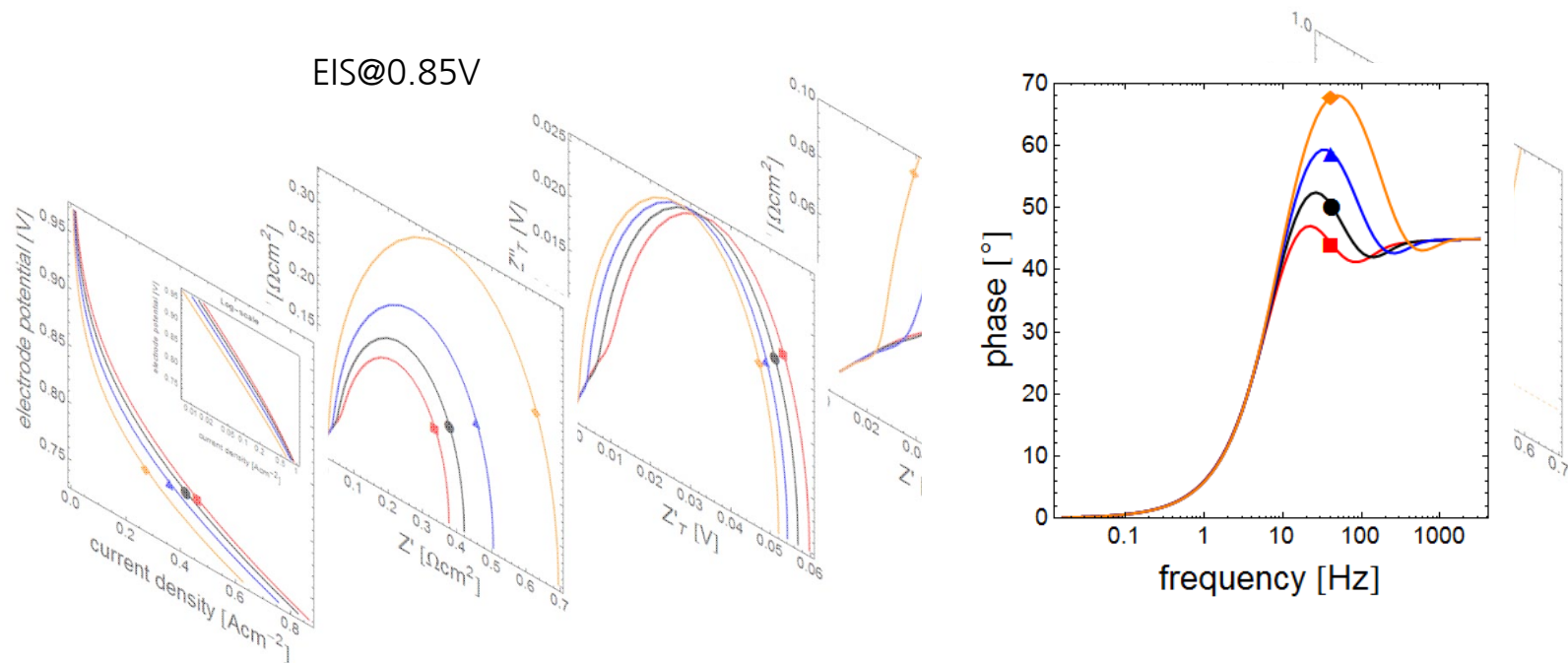
Variation of catalyst layer thickness

- Impedance as Nyquist-Plot at high frequencies
 - Linear branch
 - Thicker CL layer = longer branch



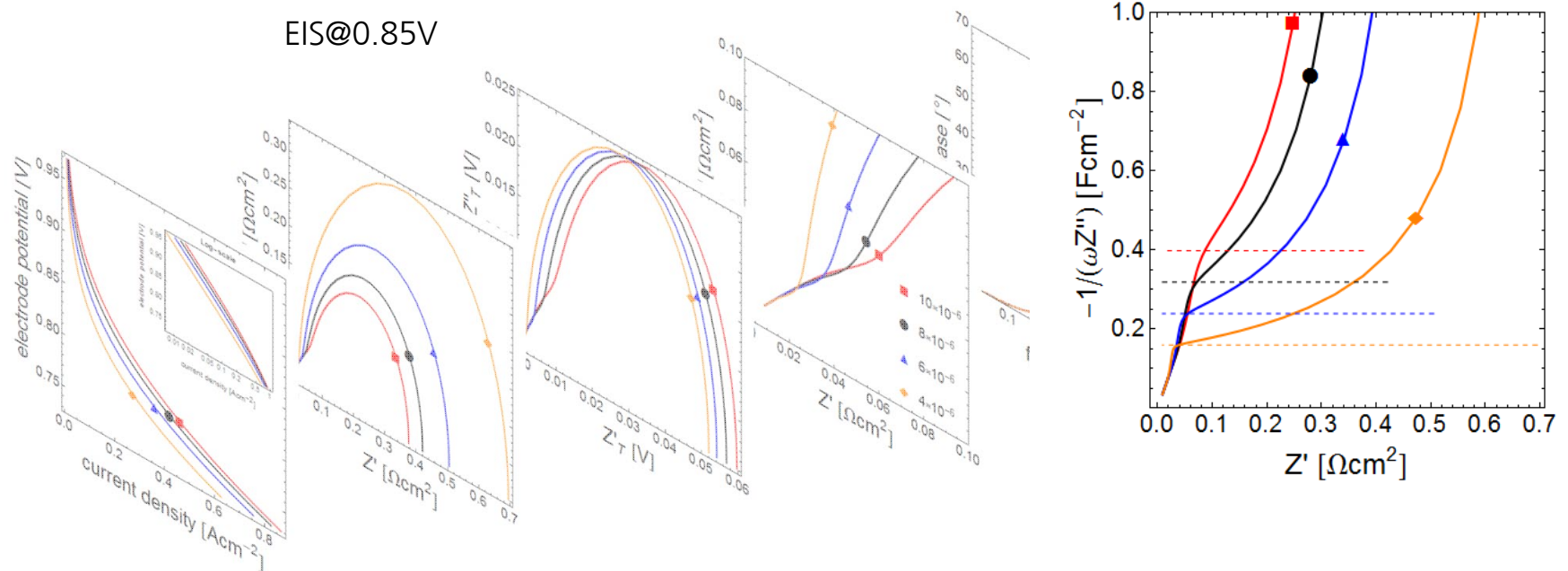
Variation of catalyst layer thickness

- Impedance as Bode-Plot (only phase)
 - Linear branch shows 45°-phase



Variation of catalyst layer thickness

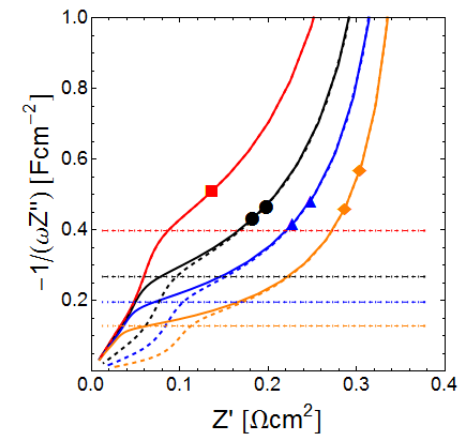
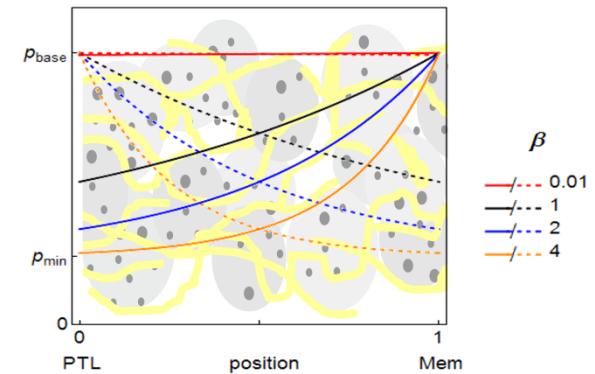
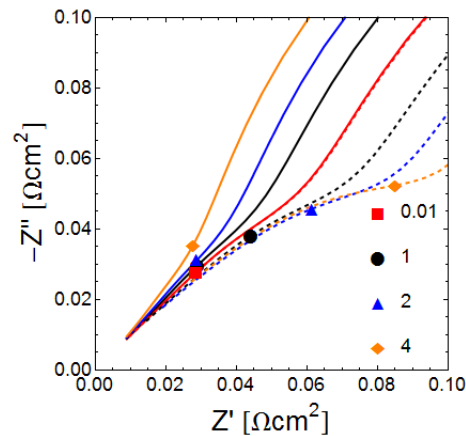
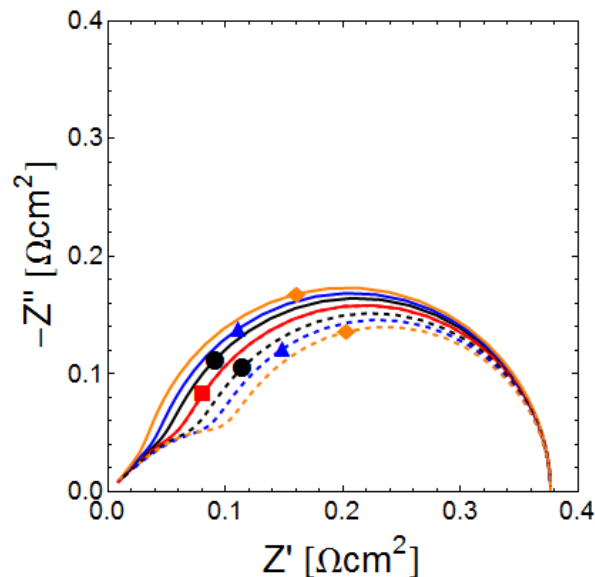
- Capacity-Plot ($1/\omega Z''$ vs Z')
 - When the perturbation completely penetrates the CL, the curve deviates from the linear branch



Distributed double-layer capacitance

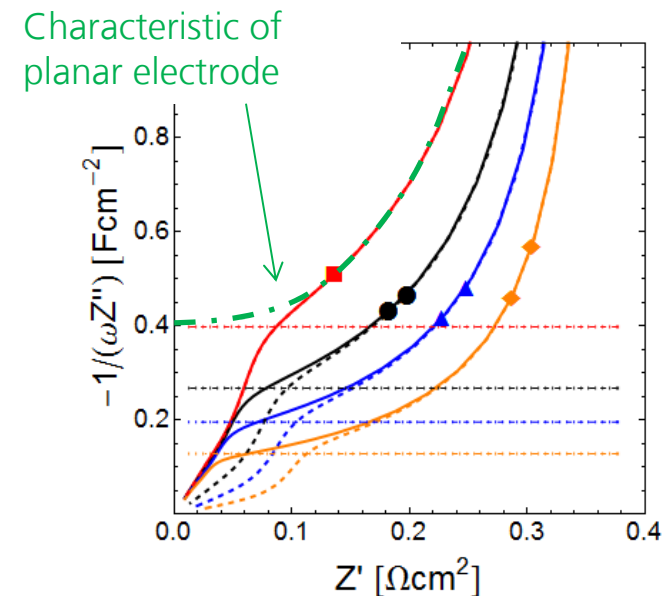
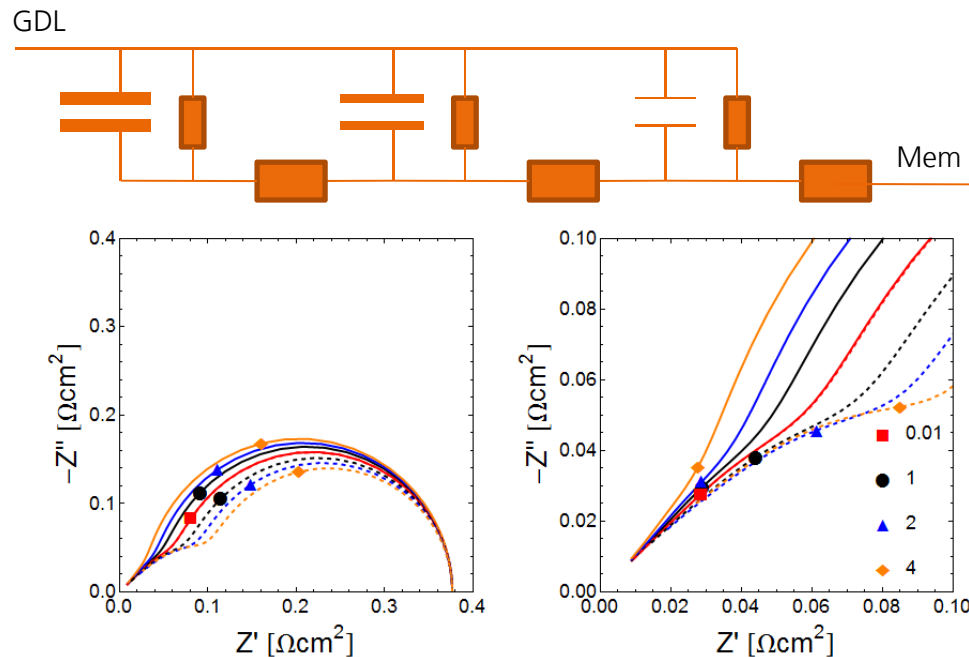
■ Impedance spectrum

- No impact on LFR → no charging currents at steady-state
- Depressed impedance arc



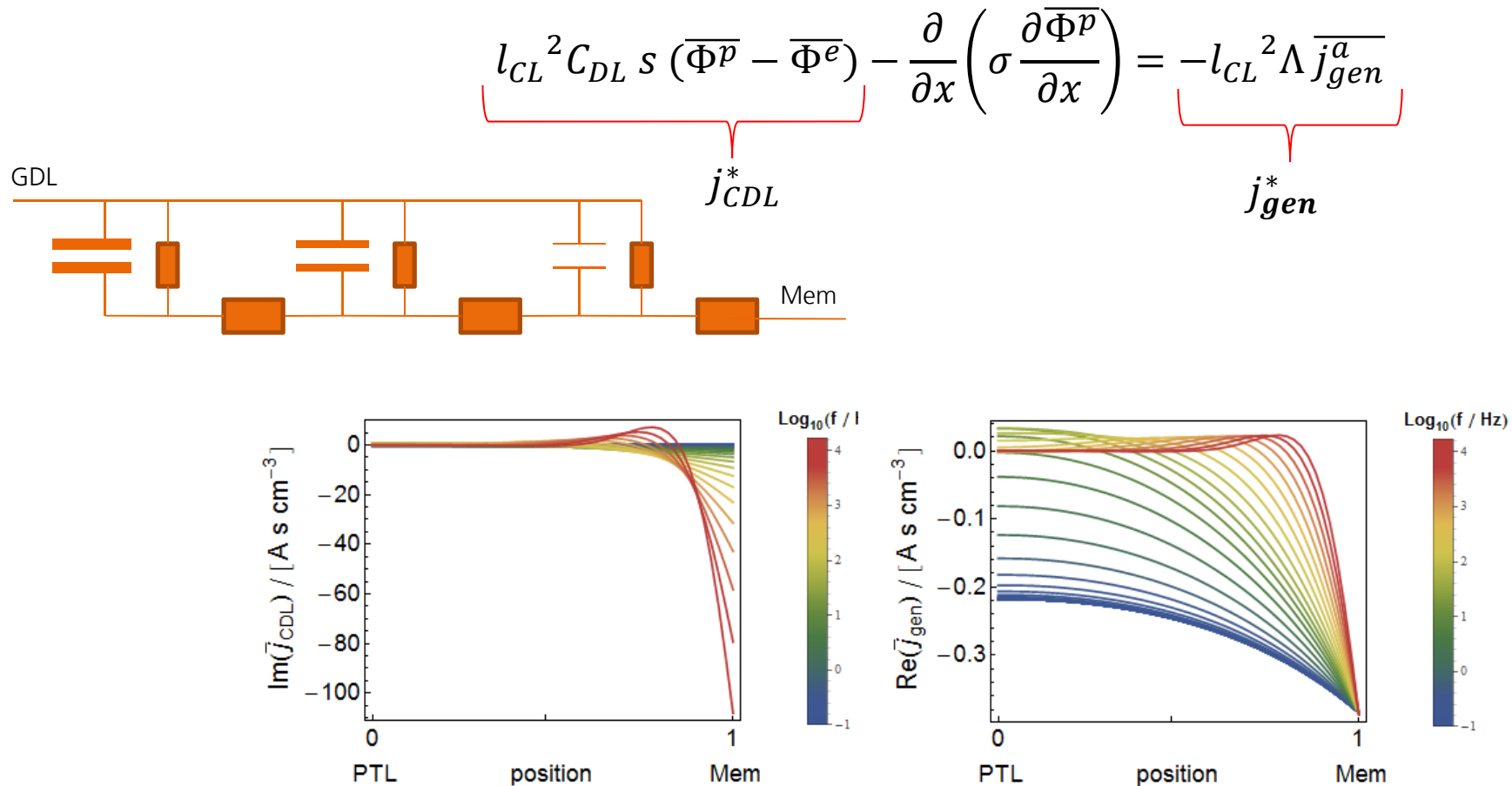
Distributed double-layer capacitance

- Capacity-Plot ($1/\omega Z''$ vs Z')
 - Turning point still defines the total electrode double-layer capacity
 - Convex shape in the high frequency range



Distributed double-layer capacitance

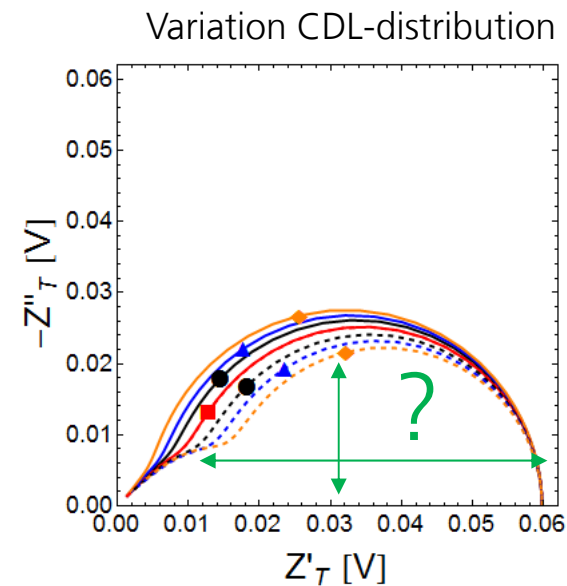
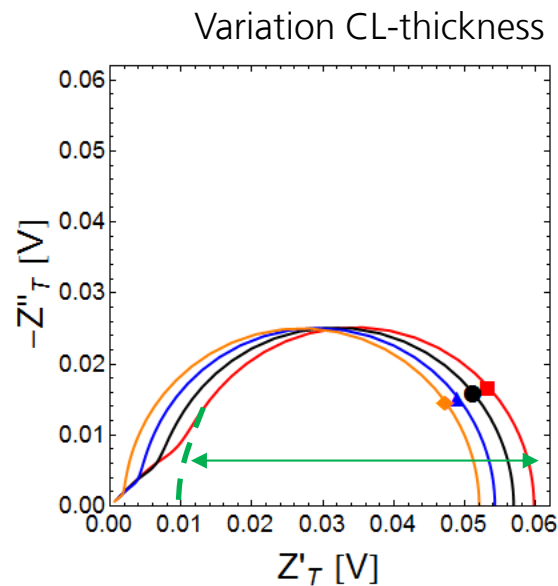
■ Penetration depth



Distributed double-layer capacitance

■ Tafel impedance

- Tafel slope can not be extracted easily by the height or diameter of the spectra



Decreasing double-layer capacitance and protonic conductivity profile towards membrane

- Theoretical consideration
 - Derivation of divergence leads to additional term

$$l_{CL}^2 C_{DL} s (\overline{\Phi^p} - \overline{\Phi^e}) - \frac{\partial}{\partial x} \left(\sigma \frac{\partial \overline{\Phi^p}}{\partial x} \right) = -l_{CL}^2 \Lambda \overline{j_{gen}^a}$$

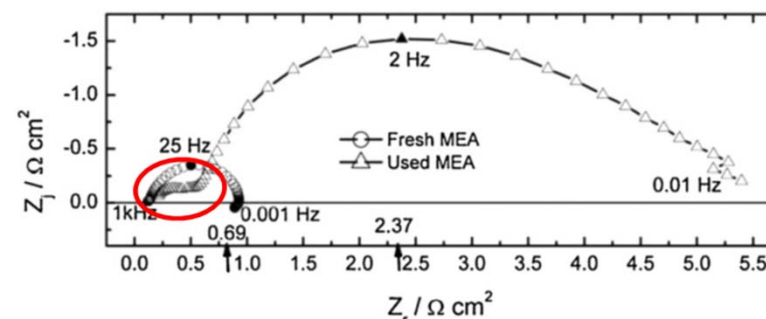
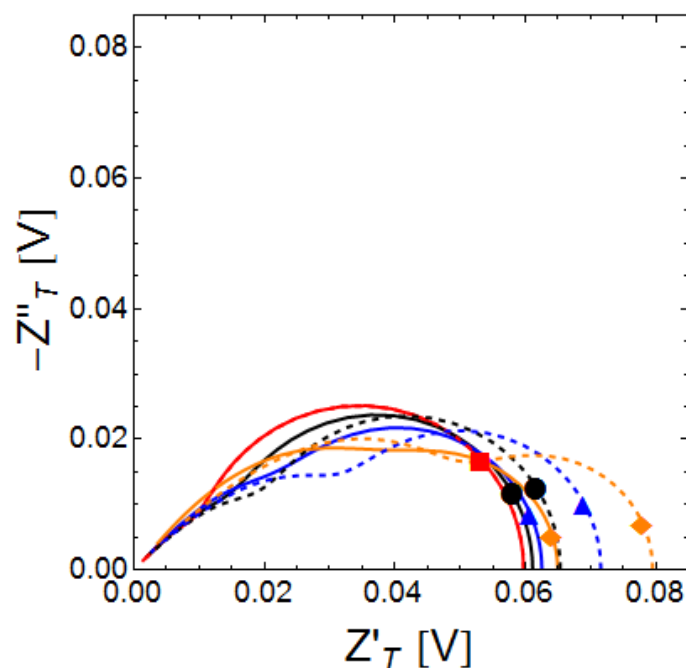
$$\underbrace{l_{CL}^2 C_{DL} s (\overline{\Phi^p} - \overline{\Phi^e})}_{j_{CDL}^*} - \underbrace{\left(\frac{\partial}{\partial x} \sigma \right) \left(\frac{\partial \overline{\Phi^p}}{\partial x} \right)}_{j_{para-Profile}^*} - \underbrace{\sigma \left(\frac{\partial^2 \overline{\Phi^p}}{\partial x^2} \right)}_{j_{divergence}^*} = \underbrace{-l_{CL}^2 \Lambda \overline{j_{gen}^a}}_{j_{gen}^*}$$

New Term

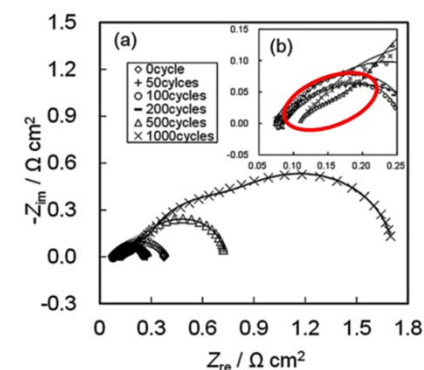
Decreasing double-layer capacitance and protonic conductivity profile towards membrane

■ Tafel impedance

- Dependent on the parameter profile the spectra separates into a low and high frequency arc.



S.K. Roy, H. Hagelin-Weaver, M.E. Orazem, Journal of Power Sources 196 (2011)



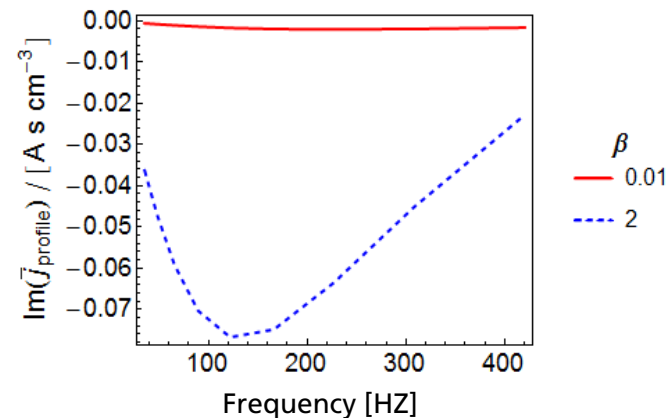
H. Nara, S. Tominaka, T. Momma, T. Osaka, Journal of The Electrochemical Society 158 (2011)

Origin of the separation into high/low frequency arc

- Comparison between homogeneous (solid) and non-homogeneous CL-properties: $\beta_\sigma = \beta_{\text{CDL}} = 2$ (dashed)
- Charge balance equation

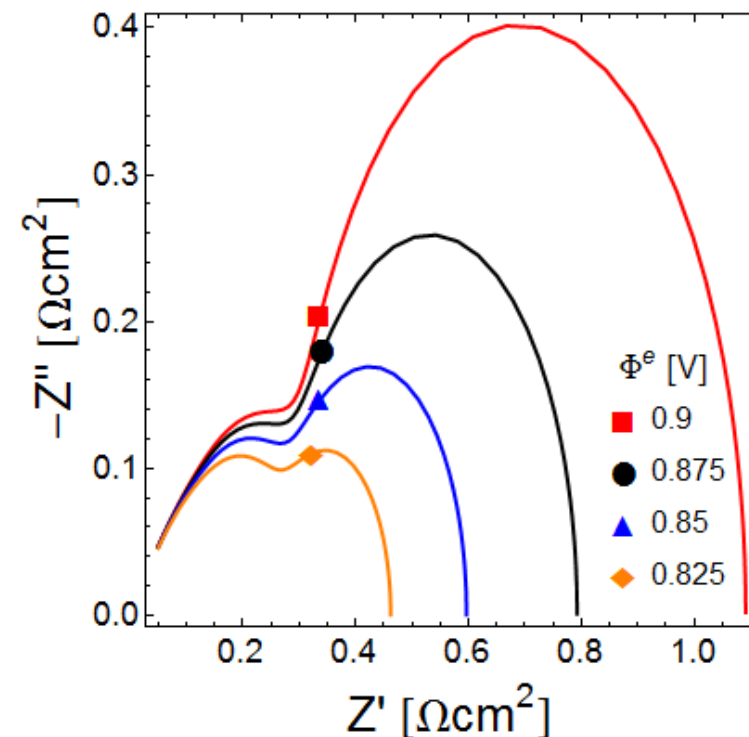
$$l_{CL}^2 C_{DL} s (\overline{\Phi^p} - \overline{\Phi^e}) - \underbrace{\left(\frac{\partial}{\partial x} \sigma \right) \left(\frac{\partial \overline{\Phi^p}}{\partial x} \right)}_{\text{Additional term}} - \sigma \left(\frac{\partial^2 \overline{\Phi^p}}{\partial x^2} \right) = -l_{CL}^2 \Lambda \overline{j_{gen}^a}$$

→ Additional term shows minimum, which is responsible for the separation



Impact of the electrode potential on the low frequency arc

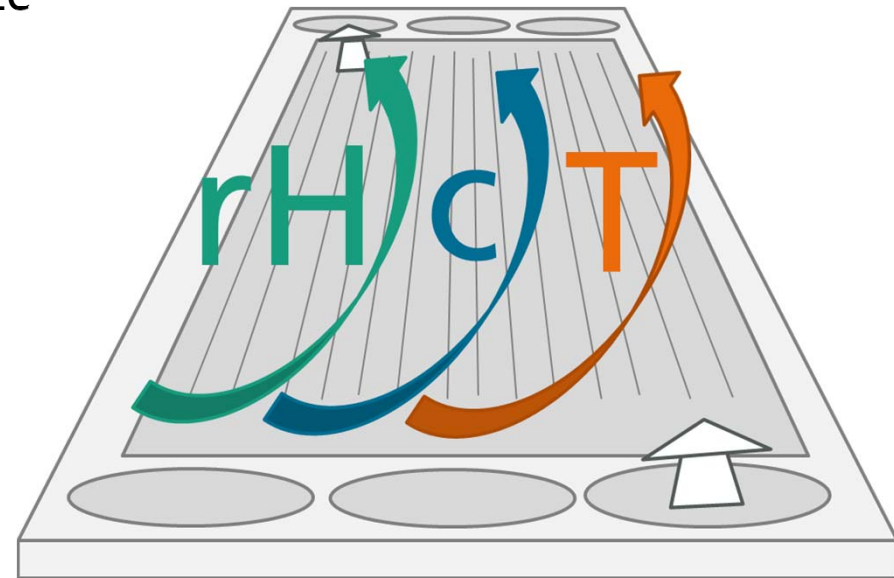
- Distributed double-layer capacitance
$$p(y) = p_{base}(\alpha + (1 - \alpha)e^{-\beta \cdot \tilde{y}})$$
- Low frequency arc decreases with decreasing potential
 - Charge transfer resistance
 - No mass transport resistance



Low frequency arc

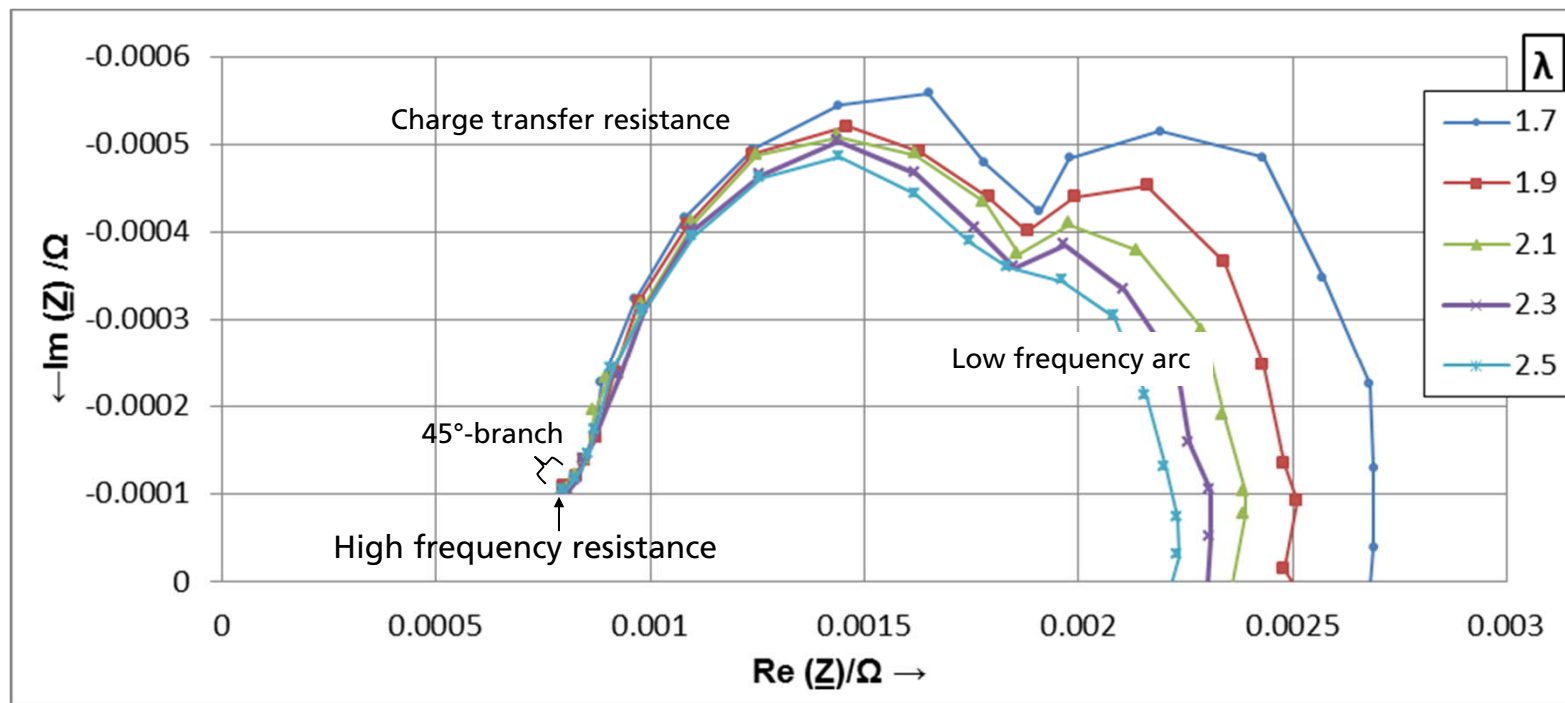
Impedance measurement at „normal“ flow conditions

- What means „normal“ in this context?
 - Non-excessive stoichiometry
 - Inhomogeneous conditions over active area
 - Cell with technical relevant size
 - Real stack hardware



How to interpret the low-frequency arc at „normal“ flow conditions

- Large impact on flow conditions → in-plane effects have to be considered



Low-frequency arc: Insights by spatially resolved EIS measurements

- Multi-Channel-Characterization-System (MCCS)



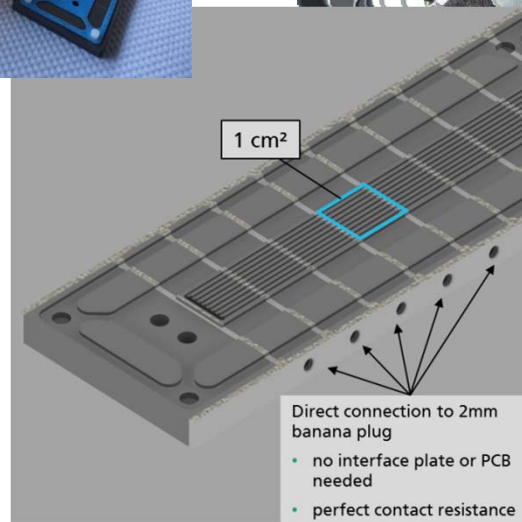
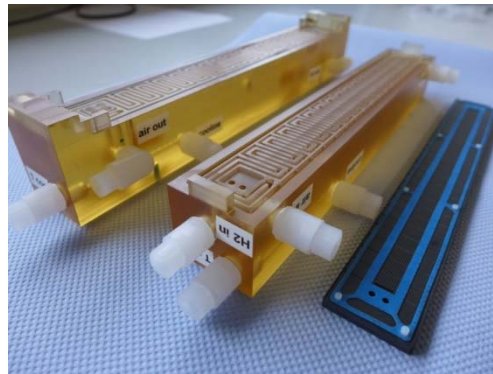
- Segmented Along-the-channel-Cell



Low-frequency arc: Insights by spatially resolved EIS measurements

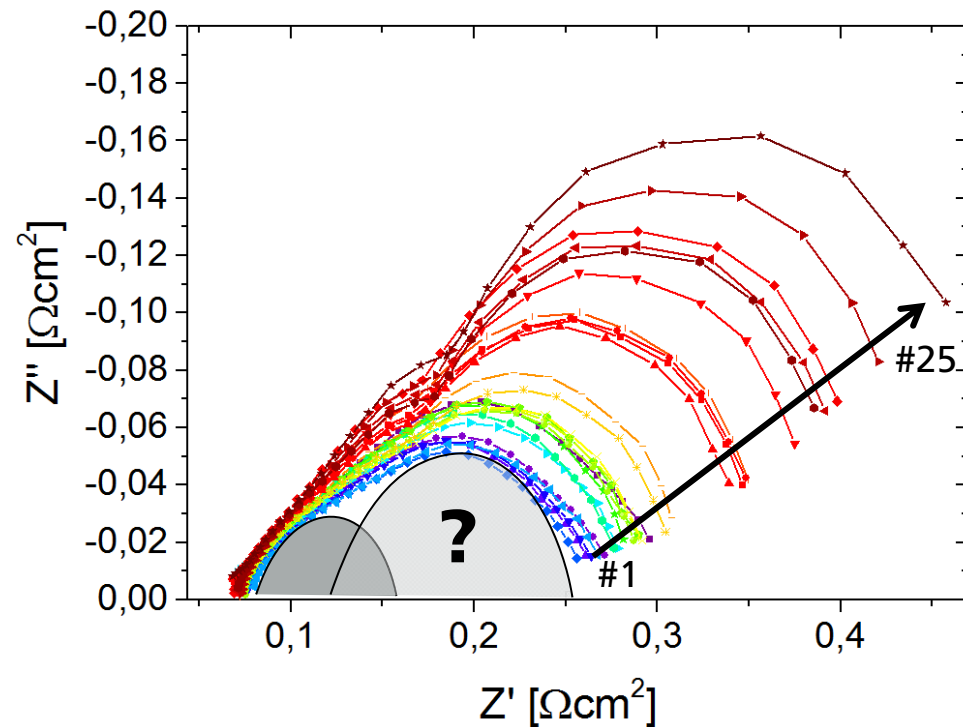
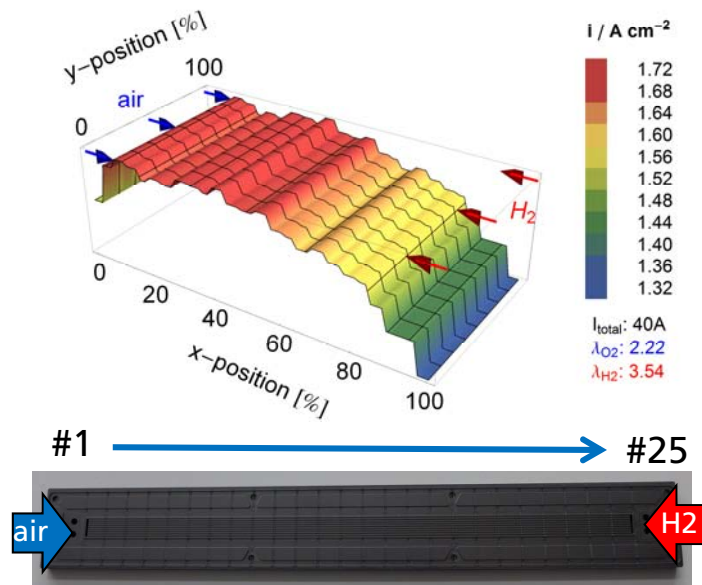
■ Segmented Along-the-channel-Cell

- 25 segments
- Size: 1 cm²
- 9 Channel á 25cm length
- Land/channel width 0.45/0.55mm



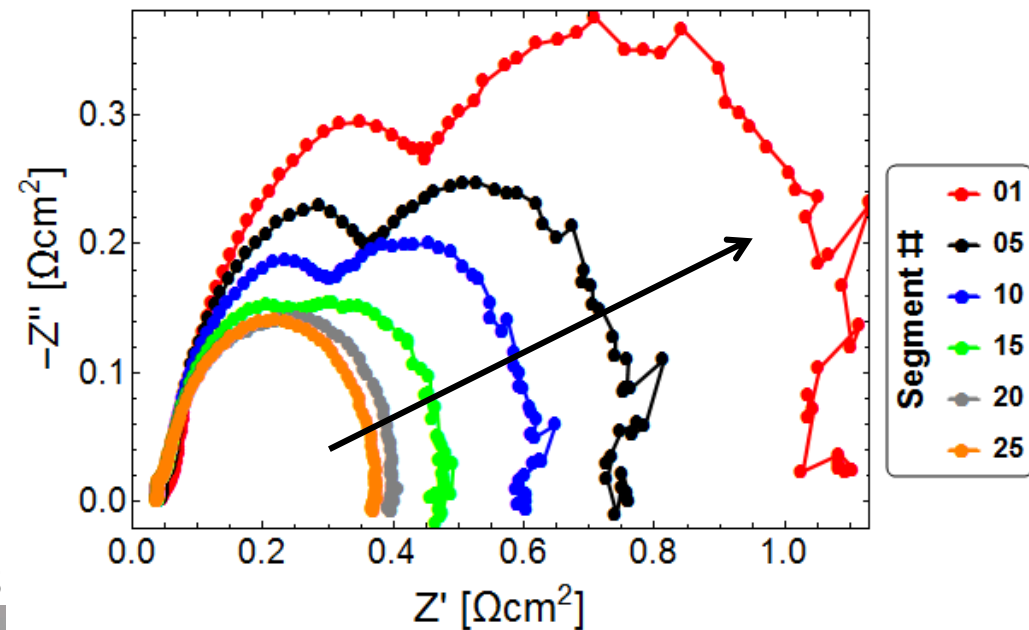
Current distribution and evolution of impedance spectra downstream the channel

- Current generation decreases from inlet to outlet ($I_{\text{total}}=40\text{A}$)
 - Low frequency arc increases
- current density @ 0.54 V



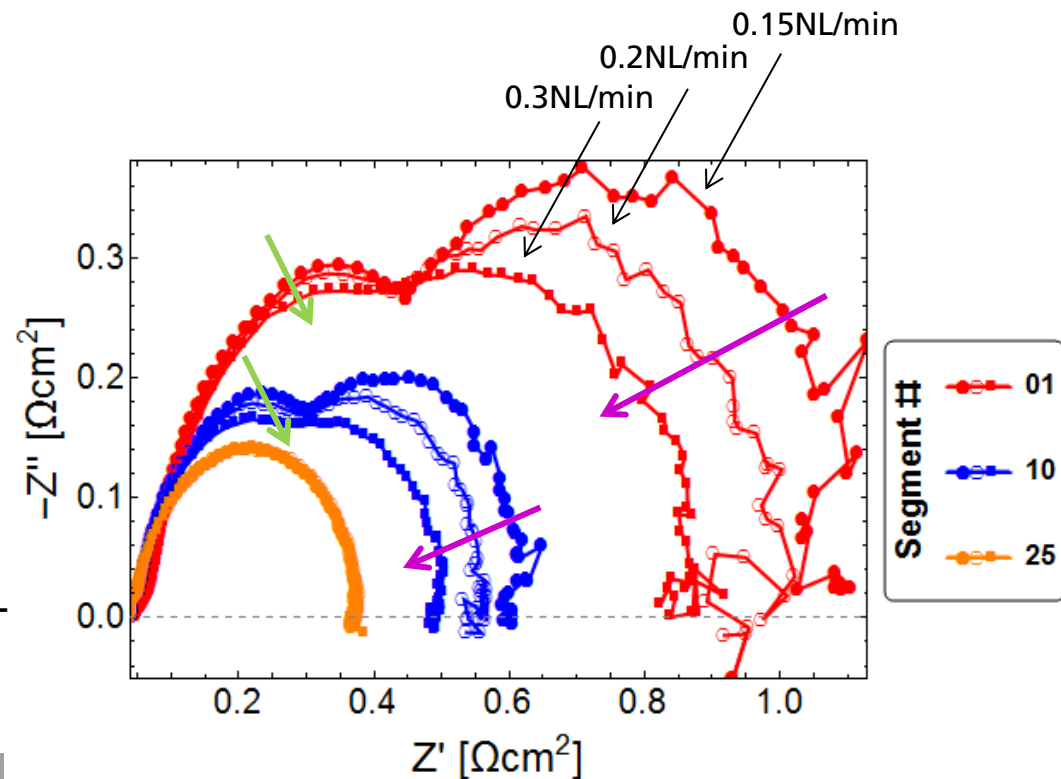
Current distribution and evolution of impedance spectra downstream the channel

- EIS @ low current density ($I_{\text{total}} < 3\text{A}$)
- Even at low current density values and „normal“ flow conditions a low-frequency arc appears

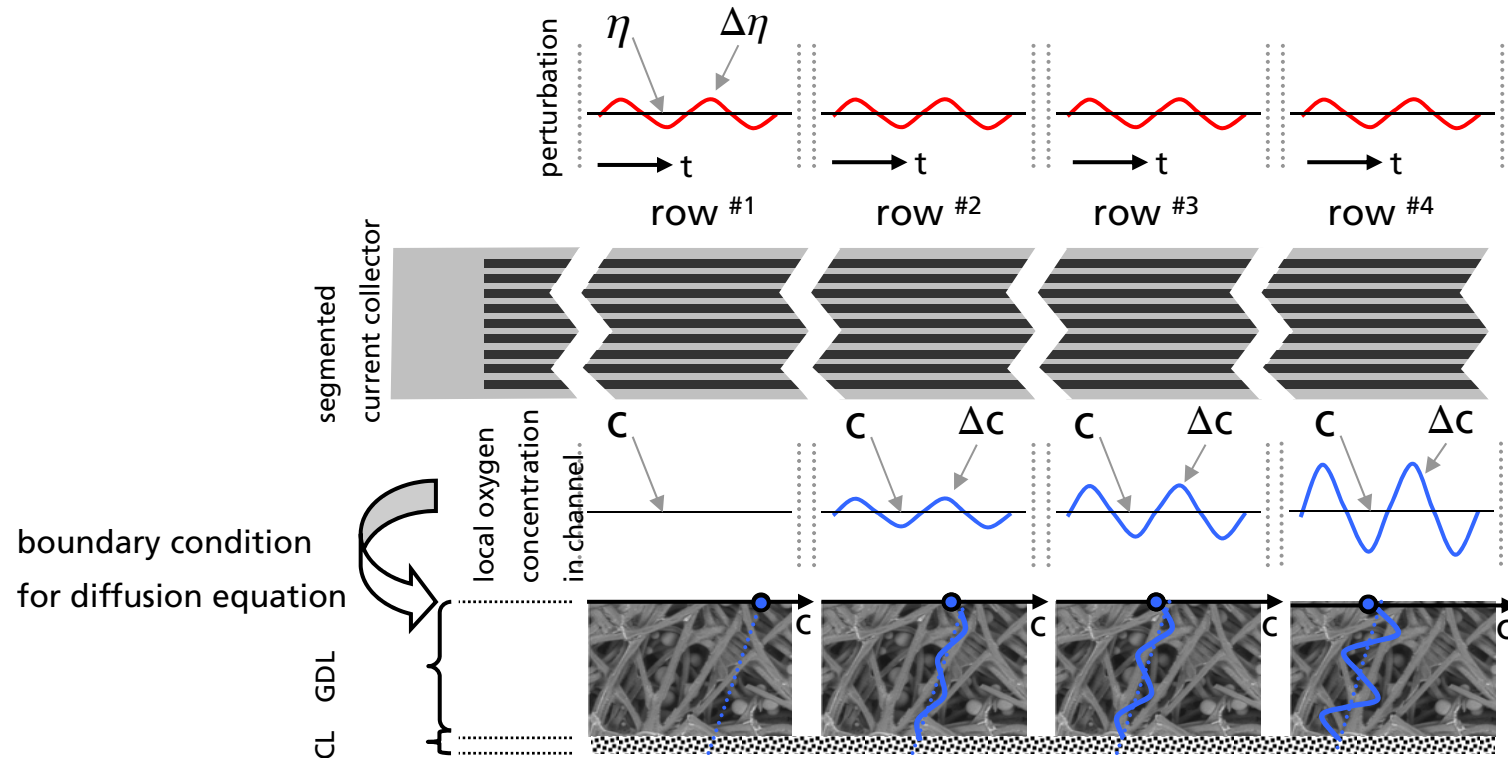


Current distribution and evolution of impedance spectra downstream the channel

- Even at low current density values and „normal“ flow conditions a low-frequency arc appears
- Increasing flow rate
 - Does not impact air inlet segment
 - Has a **small** impact on the high frequency arc
 - Effects **strongly** the low-frequency arc



What is the origin of the low-frequency arc?

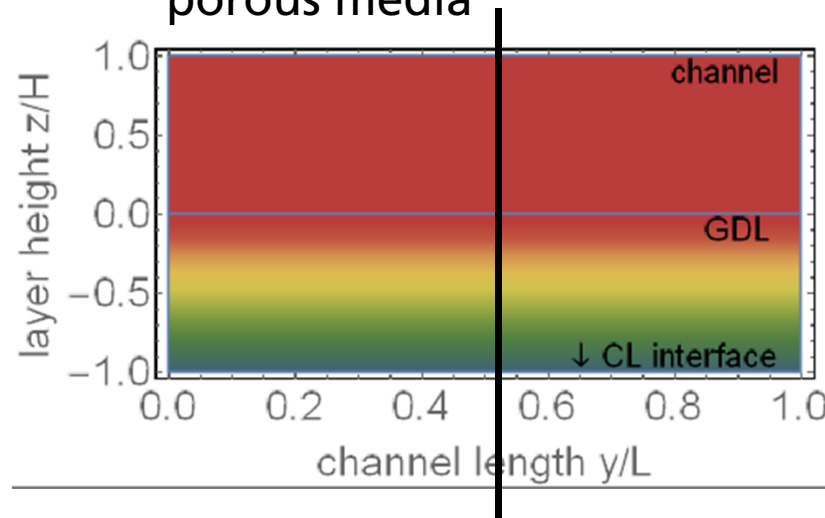


current per segment: $i_{\text{seg}} = i_0 c \exp(\eta/b)$

current response: $\Delta i_{\text{seg}} = i_0 \exp(\eta/b) (\Delta c + c \frac{\Delta \eta}{b}) - C_{\text{DL}} d_t \Delta \eta$

What is the origin of the low-frequency arc?

- Differential cell
 - High stoichiometry → no concentration gradient
 - Oscillating concentration in porous media

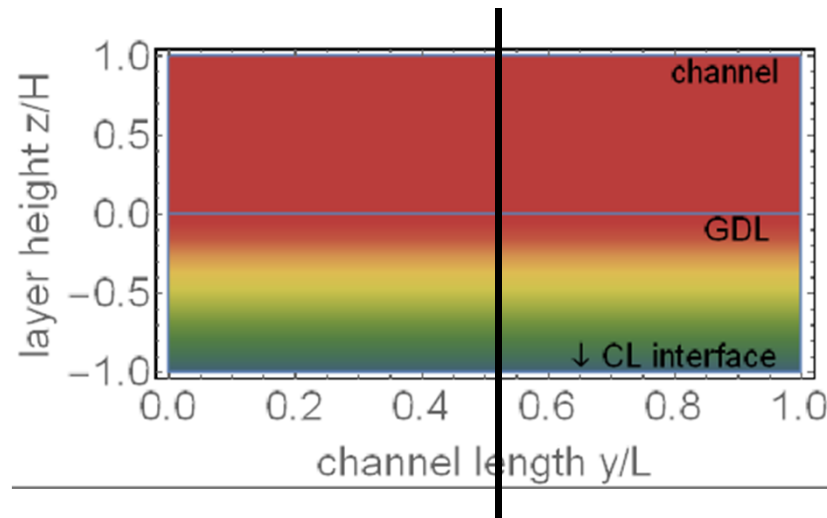


← Fix boundary condition
for oxygen concentration
→ Warburg impedance

1D-cut is representative for whole cell

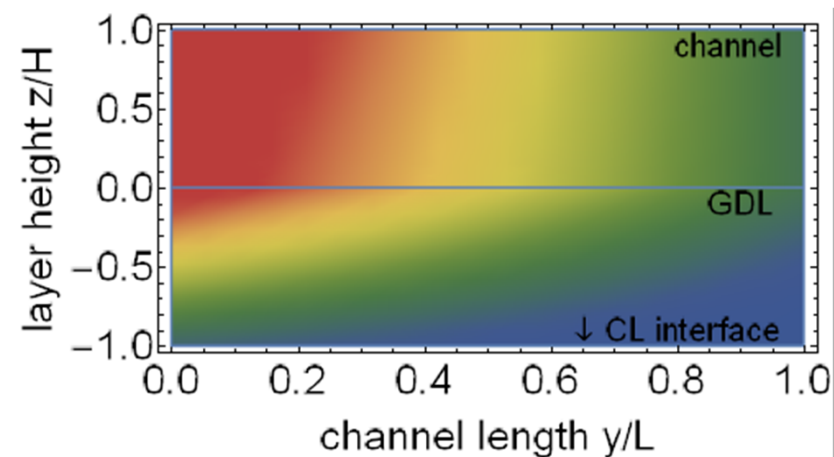
What is the origin of the low-frequency arc?

■ Differential cell



■ Non-differential cell

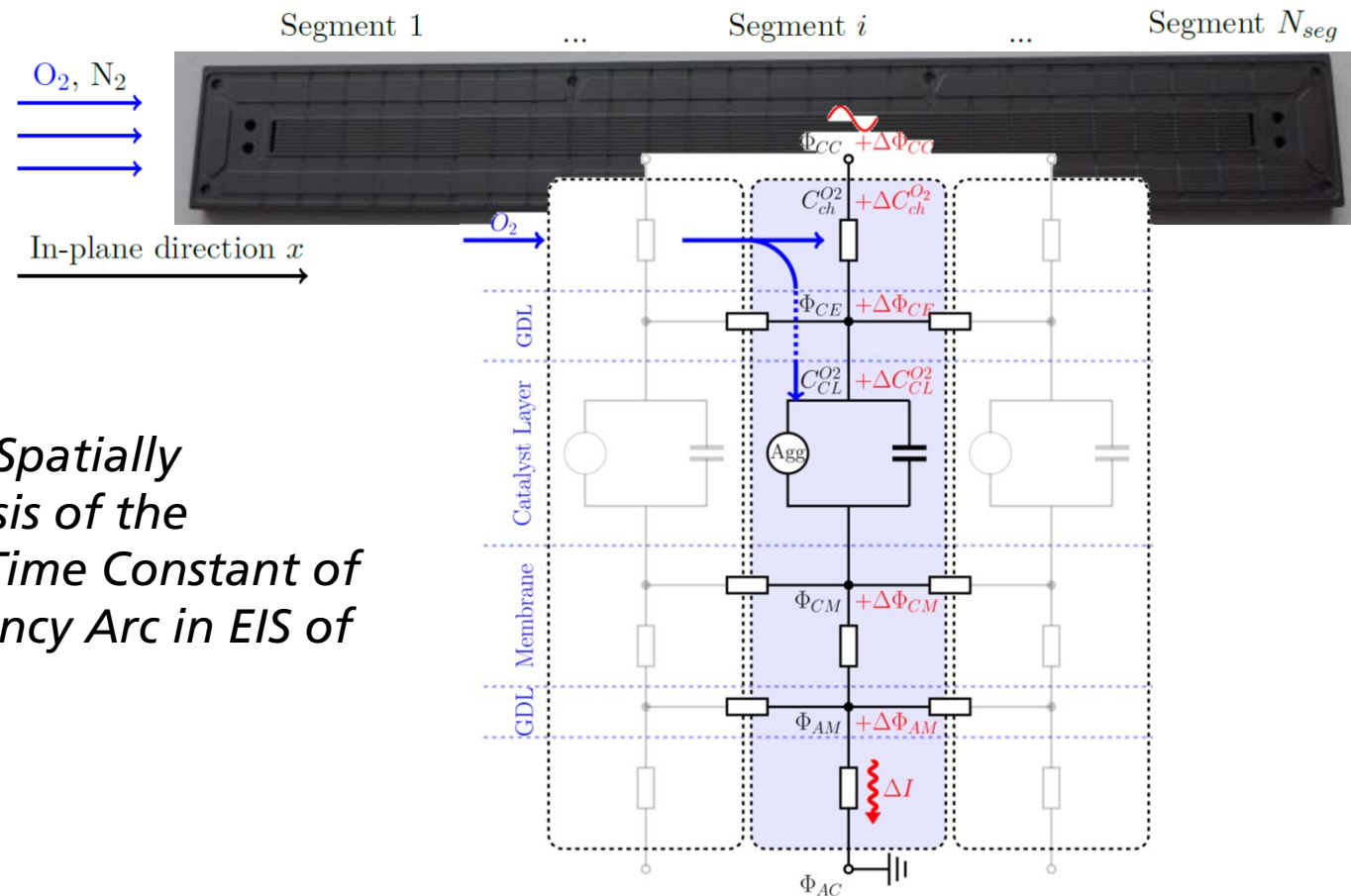
- „normal“ stoichiometry → concentration gradient present
- c_{O_2} oscillates also in-plane



Numerical model available that accounts for the oxygen dynamics in through- as well as in-plane direction

■ See poster:

Scherzer et al., *Spatially Resolved Analysis of the Characteristic Time Constant of the Low-frequency Arc in EIS of PEMFC*



Analytical cathode EIS model developed by Kulikovsky et al. for small current density values

- Negligible steady-state gradients in the CCL

- $\leq 100 \text{ mA/cm}^2$

$$J \ll \min \left\{ j_p = \frac{\bar{\sigma}_p b}{l_t}, \quad j_{ox} = \frac{4F D_{ox} c_1}{l_t} \right\}$$

- Faradaic and proton transport impedance

- $J_{0,1}$: Bessel function 1th/2nd

$$Z_{ct+p} = \frac{l_t}{\sigma_p} \left(\frac{2}{\beta \zeta} \right) \frac{J_1(\zeta) Y_0(\phi) - J_0(\phi) Y_1(\zeta)}{J_0(\phi) Y_0(\zeta) - J_0(\zeta) Y_0(\phi)}$$

$$\phi = \exp \left(\frac{\beta}{2} \right) \zeta, \quad \zeta = \frac{2}{\beta} \sqrt{-\frac{j_0 l_t}{\sigma_0 b} - i \frac{\omega C_{dl} l_t^2}{\sigma_0}}$$

- Impedance due to oxygen transport in CCL

$$Z_{ox} = \frac{b (1 - \tilde{Z}_W)}{j_0 \left(\tilde{Z}_W - \frac{\omega^2}{\omega_{ct}^* \omega_0^*} + i \omega \left(\frac{1}{\omega_{ct}^*} + \frac{1}{\omega_0^*} \right) \right) \left(1 + \frac{i \omega}{\omega_{ct}^*} \right)}$$

$$\omega_0^* = \frac{j_0}{4F c_1 l_t}, \quad \omega_{ct}^* = \frac{j_0}{C_{dl} b l_t}, \quad \tilde{Z}_W = \frac{\tanh \left(\sqrt{(j_0 + i 4F c_1 l_t \omega) / j_{ox}} \right)}{\sqrt{(j_0 + i 4F c_1 l_t \omega) / j_{ox}}}$$

Analytical cathode EIS model developed by Kulikovsky et al. for small current density values

- Impedance due to oxygen transport in GDL and channel

$$Z_{gdl+c} = -\frac{l_t/\sigma_0}{\varphi \sin \varphi} \left(\frac{c_1^0 \tilde{\eta}_1^1}{c_1^1 j_0} \varphi^2 - 1 \right)^{-1}$$

Perturbation amplitude of the oxygen concentration at the GDL/CL interface, which is a function of position

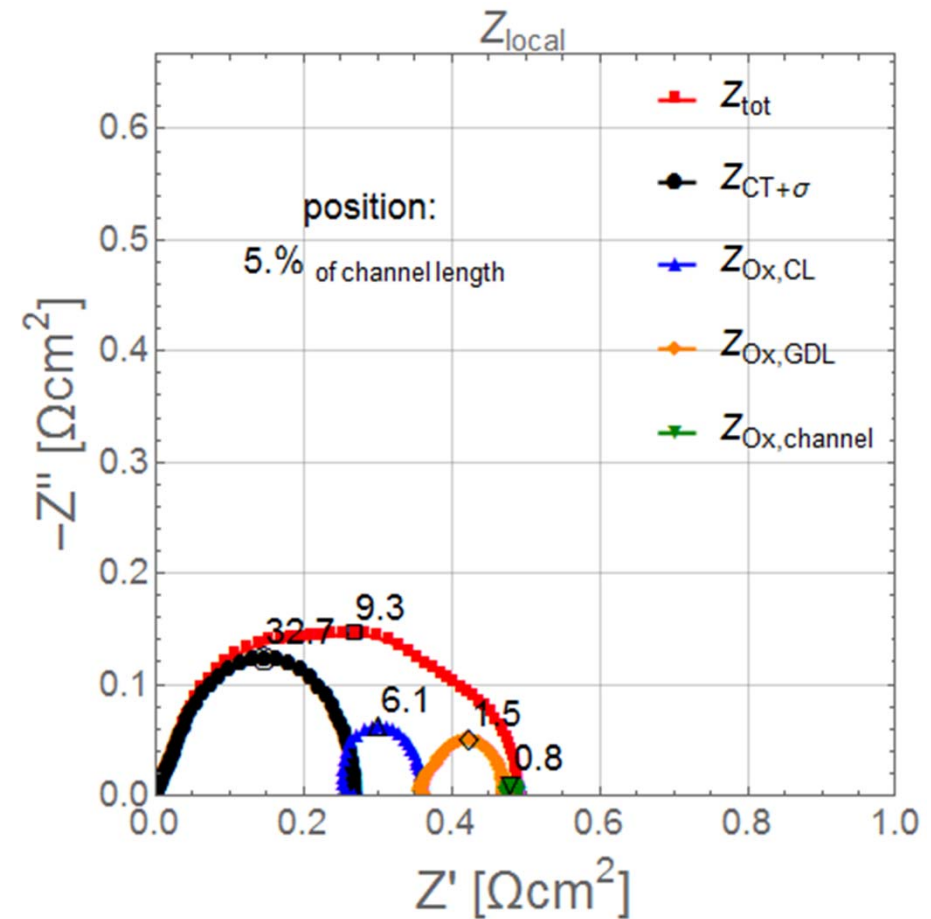
- Derivation of the different impedance contribution can be found in

T. Reshetenko and A. Kulikovsky. Impedance spectroscopy study of the PEM fuel cell cathode with nonuniform nafion loading. *J. Electrochem. Soc.*, 164:E1–E6, 2017. doi: 10.1149/2.0041711jes.

A. A. Kulikovsky. A simple physics-based equation for low-current impedance of a PEM fuel cell cathode. *Electrochimica Acta*, 196:231–235, 2016. doi: 10.1016/j.electacta.2016.02.150.

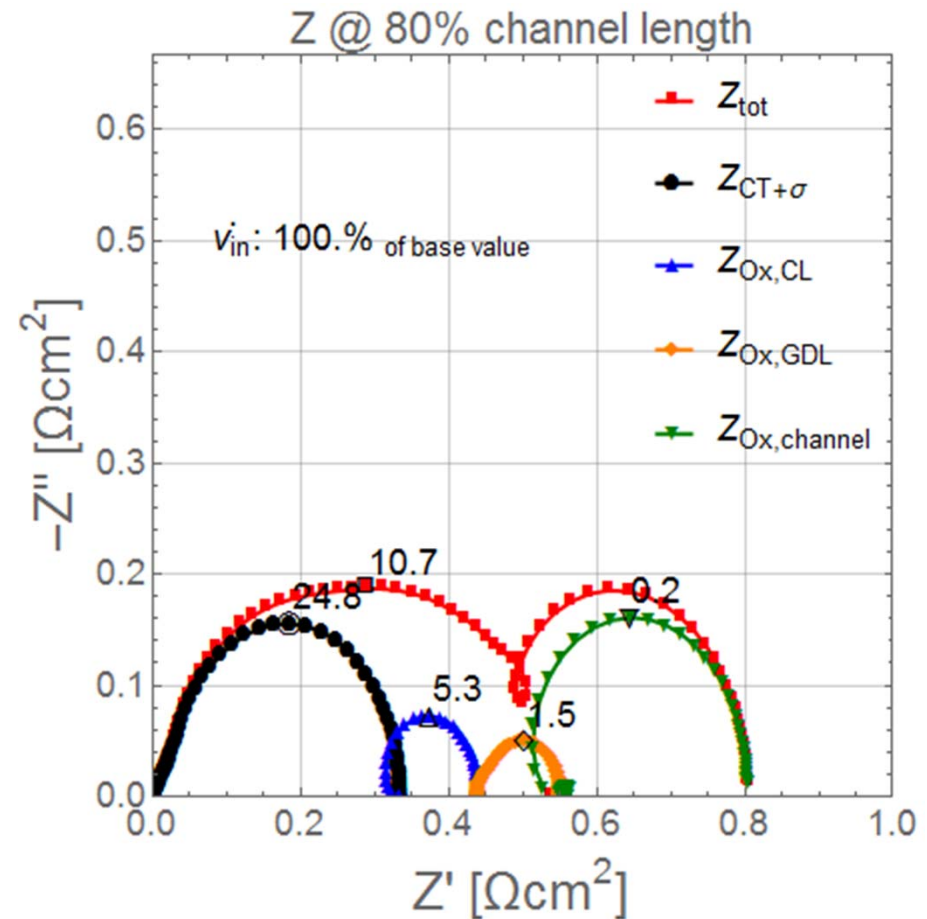
A. Kulikovsky and O. Shamardina. A model for PEM fuel cell impedance: Oxygen flow in the channel triggers spatial and frequency oscillations of the local impedance. *J. Electrochem. Soc.*, 162:F1068–F1077, 2015. doi:10.1149/2.0911509jes.

- Impact of position
 - Increase of impedance spectra is dominated by channel impedance



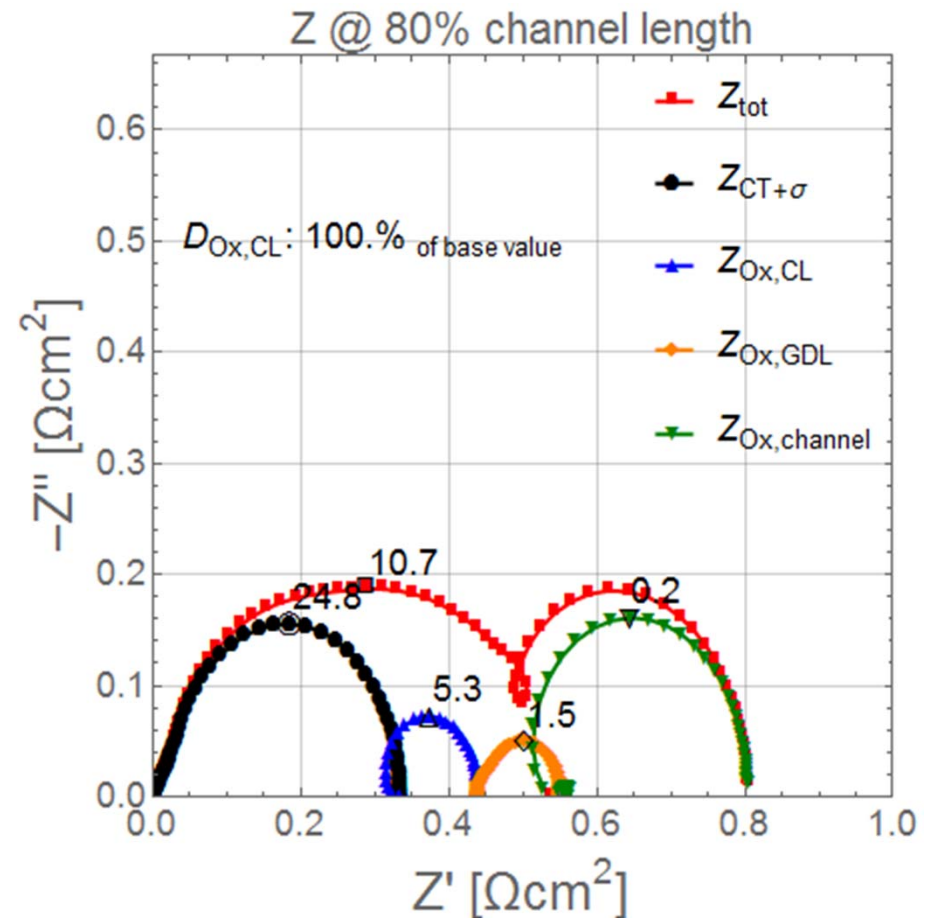
Some examples of the spatially resolved EIS model according to Kulikovsky et al.

- Impact of the flow rate / gas velocity
 - Inlet flow rate dominates the channel impedance
 - Small impact on high frequency arc (similar to experiment)



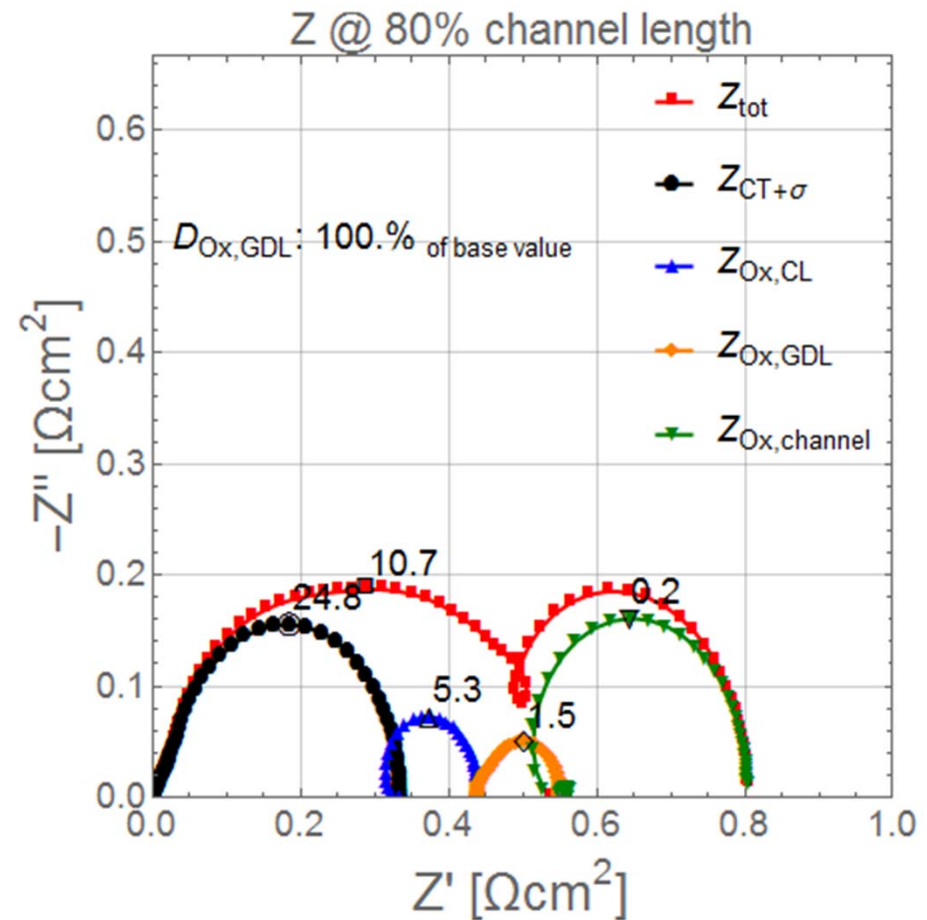
Some examples of the spatially resolved EIS model according to Kulikovsky et al.

- Impact of oxygen diffusivity in CCL
 - only $Z_{\text{Ox,CL}}$ is changing



Some examples of the spatially resolved EIS model according to Kulikovsky et al.

- Impact of oxygen diffusivity in GDL
 - all mass transport related impedances are affected



Conclusion

- Impedance spectroscopy is a powerful characterization method for analysing fuel cells
- Dependent on the cell hardware and operating conditions, the spectrum shows different features that has to be interpreted carefully
 - Inhomogeneous catalyst layer properties can result in non-expected characteristics
 - In-plane effects have to be considered in non-differential cell measurements
- By means of spatially resolved EIS measurements the mass transport impedances can better get extracted

Thank You Very Much for Your Attention!



Dr. Dietmar Gerteisen
Fraunhofer Institute for Solar Energy Systems ISE

Tel.: +49 761 4588 5205

Fax: +49 761 4588 9230

Dietmar.gerteisen@ise.fraunhofer.de

www.h2-ise.com